Catena 193 (2020) 104642

Contents lists available at ScienceDirect

Catena

journal homepage: www.elsevier.com/locate/catena

Phytoliths as paleopedological records of an histosol-cambisol-ferralsol sequence in Southeastern Brazil

Eduardo Carvalho da Silva Neto[a], Marcos Gervasio Pereira[a,*], Lúcia Helena Cunha dos Anjos[a], Marcia Regina Calegari[b], Antônio Carlos Azevedo[c], Jolimar Antonio Schiavo[d], Luiz Carlos Ruiz Pessenda[e]

[a] Universidade Federal Rural do Rio de Janeiro, Departamento de Solos, Seropédica, Rio de Janeiro, Brazil
[b] Universidade Estadual do Oeste do Paraná, Departamento de Geografia, Marechal Cândido Rondon, Paraná, Brazil
[c] Universidade de São Paulo, Escola Superior de Agricultura "Luiz de Queiroz", Departamento de Ciência do Solo, Piracicaba, São Paulo, Brazil
[d] Universidade Estadual de Mato Grosso do Sul, Departamento de Solos, Aquidauana Mato Grosso do Sul, Brazil
[e] Centro de Energia Nuclear na Agricultura, Universidade de São Paulo, Laboratório de^{14}C, Piracicaba, São Paulo, Brazil

ARTICLE INFO

Keywords:
Tropical catena
Polygenetic soils
Soil formation
Mountain soils

ABSTRACT

Soils can preserve numerous proxies that provide highly useful data on ancient climates or environments. In this study we hypothesized that analysis of the pedological cover combining soil phytolith assemblages and pedological, geochemical and isotopic analyses ($\delta^{13}C$ and ^{14}C) allows the reconstruction of events associated with the soil-landscape relationship at a toposequence scale. Soil profiles were collected from a toposequence in the upper montane environment of *Mantiqueira* Range, *Espírito Santo* State, in the Southeastern region of Brazil. Samples were collected by horizon/layer for pedological and geochemical analysis, and by depth, at 10-cm intervals, for phytolith and carbon (C) isotope (^{14}C and $\delta^{13}C$) analysis. The soils are characterized by high organic matter contents, favored by the cold and humid climate, which is typical of the upland mountainous environments of *Mantiqueira* Range. The multiproxy approach provided important information about the paleoenvironmental conditions during the pedogenesis process, allowing to establish pedochronostratigraphic correlations, that improved the understanding of soil-landscape relationships in these environments. Soil-preserved phytolith assemblages, isotopic composition ($\delta^{13}C$) and organic matter dating (^{14}C) indicated variations in the type of plant communities in the studied soils, suggesting climatic changes that influenced the soil formation and evolution. The soils experienced different pedogenesis conditions during the Late Holocene, and are, therefore, considered polygenetic soils. In summary, 3 environmental moments were identified by multiproxy analysis: **Phase I** (before −2330 cal. yr BP), hotter and drier than the current period; **Phase II** (from −2330 to −2063 cal. yr BP), colder and wetter than the current period; **Phase III** (after −2063 cal. yr BP), during which the current climate conditions were established.

1. Introduction

Soils observed today are the result of many factors that continuously change in space and time. The characteristics observed in a soil profile reflect the equilibrium of specific conditions over time intervals, and the degree of expression of these characteristics depends on the intensity and duration of the pedogenic processes. Therefore, soils can be considered archives of paleoenvironmental changes (Janzen, 2016; Targulian and Bronnikova, 2019), and pedogenesis is not only an active biogeochemical process that occurs on the earth's surface but is also a means of recording climatic information (Targulian and Goryachkin, 2011).

Pedogenic intensity is known to be strongly dependent on characteristics of the geomorphic surfaces (Curi and Franzmeier, 1984; Anjos et al., 1998; Vidal-Torrado et al., 2005). They determine intensity of soil surface wash vs. solution loss, degree of weathering, depth of solum, illuviation process, organic matter and cation accumulation. One approach for studying the variation of soils in a landscape is the structural analysis of the pedological cover (Boulet, 1978), based on the concept of catena, which is used to express the systematic and repetitive

* Corresponding author.
E-mail addresses: netocseduardo@gmail.com (E.C.d. Silva Neto), mgervasiopereira01@gmail.com (M.G. Pereira), lanjosrural@gmail.com (L.H.C.d. Anjos), marciareg_calegari@hotmail.com (M.R. Calegari), aazevedo@usp.br (A.C. Azevedo), schiavo@uems.br (J.A. Schiavo), pessenda@cena.usp.br (L.C.R. Pessenda).

https://doi.org/10.1016/j.catena.2020.104642
Received 11 January 2020; Received in revised form 14 April 2020; Accepted 28 April 2020

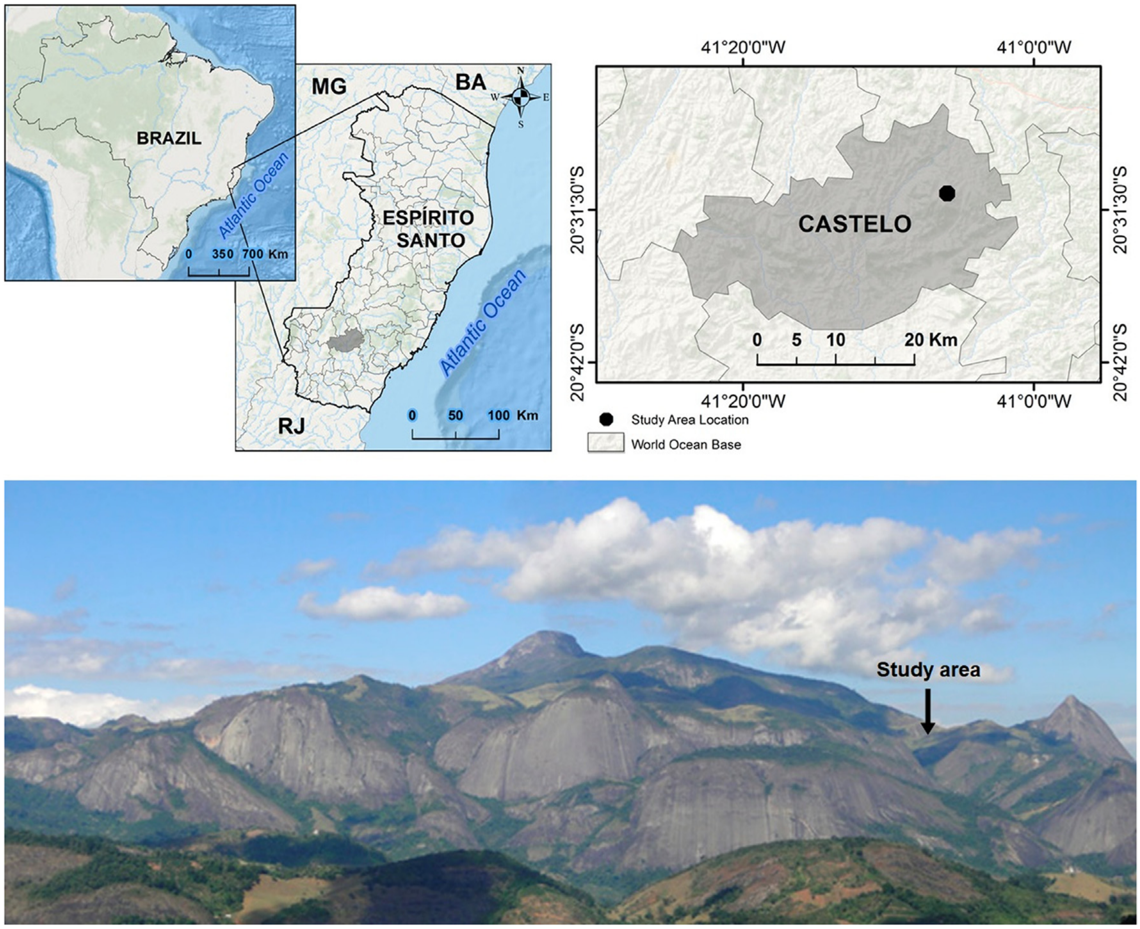

Fig. 1. Location of the study area in upper montane section of Mantiqueira Range, Espírito Santo State, SE region of Brazil. Adapted from Silva Neto et al. (2019).

distribution of soils along the slopes. According to Boulet (1978), the structural analysis of the pedological cover makes it possible to reconstruct the spatial distribution of soils along slopes. However, such a study should be performed at all available observation scales, i.e., from field macromorphology, through an optical microscopy scale, as in the micromorphology, to element distribution analysis. These different scales of analyses complement each other and allow for a more thorough study of pedogenesis (Vidal-Torrado et al., 2005).

In addition to their characteristics, soils can preserve numerous proxies that provide highly useful data on ancient climates or environments. Among them, phytoliths (silica-phytoliths) have stood out for their versatility in paleoclimatic studies. Phytoliths are amorphous silica particles that accumulate around or within plant tissue cells (Piperno, 2006), thus, they represent variable aspects of preserved plant anatomy (Neumann et al., 2019). As some morphotypes are specific to plant families and subfamilies, a set of phytoliths (phytolithic assemblage) preserved in the soil may characterize a plant community, representing a key dataset for studies aimed at reconstructing paleoenvironments. With the emergence of phytolith analysis as an important tool for answering several paleoecological and paleoclimatic questions, the number of studies related to different aspects of phytoliths has increased tremendously in the past few decades (Rashid et al., 2019). However, few studies in Brazil have aimed to reconstruct climatic conditions during pedogenesis.

The past climate of the region and of southeastern Brazil remains under debate; however, it is widely accepted that it was very unstable during the Quaternary (Pinheiro and Queiroz Neto, 2017). Multiproxy studies have been conducted in this region of Brazil to understand these environmental changes based on soil records (bioindicators) linked to pedological, geochemical and isotopic analysis (e.g., Calegari et al., 2013a; Horak-Terra et al., 2014, 2015; Chiapini et al., 2018; Silva Neto et al., 2018a, 2018b, 2019). These studies have provided important paleoenvironmental information that complements studies of soil genesis. In the classical concept of pedogenesis, soil is the product of a function (the relationship between the parent material in a topographic condition, which is subjected to different climatic conditions over time with the action of fauna and flora). With the paleoenvironmental reconstruction studies it is possible to access, to know more precisely the past vegetation composition and, from this, to infer the past climate.

Along with Sea Mountain Range, Mantiqueira Range constitutes the most outstanding orographic feature on the Atlantic edge of the South American continent, having been called, due to its escarpments, tectonic processes, faults, and marked folds, the “most tormented relief in the country”. It stands out in the Brazilian landscape because of both its impressive geomorphological features and its role in the human occupation of Brazil from the period of colonization to the present day (Vieira and Gramani, 2015). In the state of Espírito Santo a branch of the Mantiqueira Range constitutes upper montane environments highly heterogeneous, with different reliefs, and with specific temperature and humidity conditions that favor the formation of soils with high organic matter (SOM) content, which can potentially be used for paleopedological studies. However, only a few studies relating to soil characterization and genesis have been developed to explain the evolution of soil and landscapes in these upper montane conditions (Pereira et al., 2012; Silva Neto et al., 2019).

Thus, we hypothesized that the study of the pedological cover combining soil phytolith assemblages and pedological, geochemical and isotopic analysis ($\delta^{13}C$ and ^{14}C) allows the reconstruction of events associated with the soil-landscape relationship at a toposequence scale. Accordingly, the main objective of this study was to broaden our understanding of soil genesis in high montane environments of the Atlantic Forest biome in Southeastern region of Brazil, through a multiproxy study of profiles along a toposequence.

2. Materials and methods

2.1. Study area

The study area is located on a branch of Mantiqueira Range, Espírito Santo State, Southeastern region of Brazil (coordinates between 20°31′6.23″S 41°6′52.88″W and 20°29′31.28″S 41°4′43.72″W) (Fig. 1).

The Mantiqueira system straddles the southeastern coastal region of Brazil, forming a ca. 2500-km long Neoproterozoic collisional domain (Vieira and Gramani, 2015). This region is predominantly located on Precambrian basement consisting of Proterozoic to Eopaleozoic metamorphic and igneous plutonic rocks (granites and gneisses). Geomorphologically, it is characterized by an intensely dissected pattern, highlighted by large massif elevations, some exceeding 2000 m in altitude. The combined effects of tectonic events and predominantly wet climates on these rocks are noted in dissection shapes intensively oriented by cross faults, adapted escarpments, and residual faults and elevations.

The native vegetation is a mosaic of mixed rainforest components, with montane and upper montane forest species, characteristic of southern Brazil, high-altitude fields, and temperate genera, reflecting the effect of low temperatures, caused by altitude, on the floristic composition of the area. The climate is subtropical humid (Cwb, Köppen classification), 1900 $mm \cdot yr^{-1}$ annual average precipitation and 21.4 °C annual average temperature (Alvares et al., 2013). In winter, the average temperature is 16.8 °C and the average monthly rainfall is 27 mm $month^{-1}$. In summer, the average temperature is 24.6 °C and the average monthly rainfall is 187 $month^{-1}$.

A total of 3 pedons were collected along a toposequence, P1 between the summit and shoulder position, P2 on the backslope, and P3 on the footslope. They were selected from previous field records of soils with high SOM content in the area. It was presumed that these soils had high potential for paleoenvironmental studies, because the subtropical climate is relatively cold and wet, which helps to preserve SOM and phytoliths deposited in bygone eras. The sites for soil sampling where chosen from locations with the lowest degree of anthropic intervention.

2.2. Selected soils and sampling

Three soil profiles were selected following a catena at the Mantequeira Range (Fig. 2). Sample collection and description followed the guidelines for soil description outlined in (Jahn et al., 2006). The P1 profile, a Sapric Histosol, was described in a concave portion of the slope located between the summit and shoulder positions of the toposequence, and exhibited characteristics indicating impeded drainage. The histic horizon had a depth of 75 cm and the mineral horizon, Cg, showed a massive continuous structure and grayish colors, characteristic of the pedogenic process of gleization (van Breemen and Buurman, 2002; Buol et al., 2011). This process is characterized by the reduction of Fe3+ to Fe2+ by anaerobic microorganisms in the presence of SOM, primarily due to the presence of stagnant water.

In the middle section of the slope, the P2 profile, a Dystric Cambisol, had an umbric surface horizon followed by another A horizon, even darker (10YR 4/3) than the upper surface horizons (10YR 5/2 and 4/6), and also with high content of SOM, suggesting it to be a buried horizon. The presence of rock fragments immersed in the soil matrix and of a lithology different from the above horizon, as well as the aggregates with larger size and sub angular block type in the 2Ab sub horizons, indicate a lithological discontinuity above the buried horizon, most likely due to colluvium material (2Ab1 66–89 cm, and 2Ab2 89–110 cm).

The P3 profile, an Umbric Ferralsol, located in the lower section of the slope, also had subsurface horizons which were darker than the overlying horizons. Morphological analysis showed the same color, 10YR 4/2, from the surface to the A3 sub horizon (−48 cm soil depth). From this depth, the chroma value slightly decreased in the A4 (10YR 3/1) and A5 (10YR 3/2) sub horizons, which maintained the high SOC contents. No significant differences in particle-size distribution, mineralogy, structure or consistency were detected in the darker horizons, that could suggest the presence of a lithologic discontinuity. Strong evidence of bioturbation was observed in this P3, indicating very effective mixing of soil materials between horizons by the soil "engineers" fauna (e.g., earthworms, termites), transporting organic materials to deeper layers of the soil. The mixing of the horizons and the bioturbating by soil fauna could explain the homogeneous pattern with increasing soil depth.

2.3. Soil physical, physicochemical and chemical characteristics

The physical and chemical characterization of soil samples was performed according to the Manual of Methods of Soil Analysis of the Brazilian Agricultural Research Corporation (Teixeira et al., 2017). The physical analyses involved the evaluation of the percentage of fine earth fraction, naturally dispersed clay and degree of flocculation (DF), silt/clay ratio, bulk density (Ds) and particle (Dp) density, total pore volume (TPV), and granulometry of the soil.

For the physichemical characterization of samples, the pH was determined in water and in KCl at a 1:2.5 (soil:water) ratio, exchangeable calcium (Ca^{+2}), magnesium (Mg^{+2}) and aluminum (Al^{+3}) were analyzed by titration, assimilable phosphorus (P) and exchangeable potassium (K^{+}) and sodium (Na^{+}) were determined by colorimetry and flame photometry, and extractable acidity ($H^{+}+Al^{+3}$) and hydrogen (H^{+}) were assessed in a 0.025 mol L^{-1} calcium acetate solution (Teixeira et al., 2017). Soil organic carbon (SOC) was determined by wet oxidation (Teixeira et al., 2017). Total content of the main soil oxides was determined extracting these following the sulfuric acid method; results are expressed as SiO_2, Fe_2O_3, Al_2O_3, and TiO_2.

In addition, samples from the histic horizons were classified according to the Von Post decomposition scale (Santos et al., 2018), which involved squeezing a handful of wet soil, and observing the color of the extracted fluid, the nature of the plant fibers, and the residual proportion of the original sample retained in the hand. The classes (1) to (4) comprised fibric organic soil material, classes (5) and (6) hemic organic soil material, and the classes (7) to (10) sapric organic soil material (Santos et al., 2018).

Mineral crystalline phases were identified by X-ray diffractometry using the Rigaku Miniflex II, with Cu K-alpha radiation, Ni filter and graphite monochromator.

The mineral horizons samples were treated with hydrogen peroxide to eliminate organic matter substances. Sand and silt + clay fractions were separated by wet sieving, and silt and clay were separated by settlement velocity, according to the Stokes equation. Sand and silt particles were randomly mounted, while treated clay aliquots were mounted as oriented slides by smearing. The clay fraction was saturated first with K and heated at 25, 350 and 550 °C), and then with Mg and Mg with glycerol, both at 25 °C, following which it was irradiated. Diffraction patterns were interpreted according to Jackson (1975), Brown and Brindley (1980), Moore and Reynolds (1989) and the Crystallographic Open Database (COD) (Gražulis et al., 2009).

2.4. Ki and Kr indices and total elements

SiO_2, Fe_2O_3, Al_2O_3, and TiO_2 contents were extracted by sulfuric attack (H_2SO_4, 1:1), as described by Teixeira et al. (2017). The total concentration of elements was determined by X-ray fluorescence (XRF), at the Federal University of Viçosa (*Universidade Federal de Viçosa* – UFV). Soil samples (0.6 g) were treated with 5.4 g lithium tetraborate and heated to 1,100 °C until melting into pellets, using a Philips

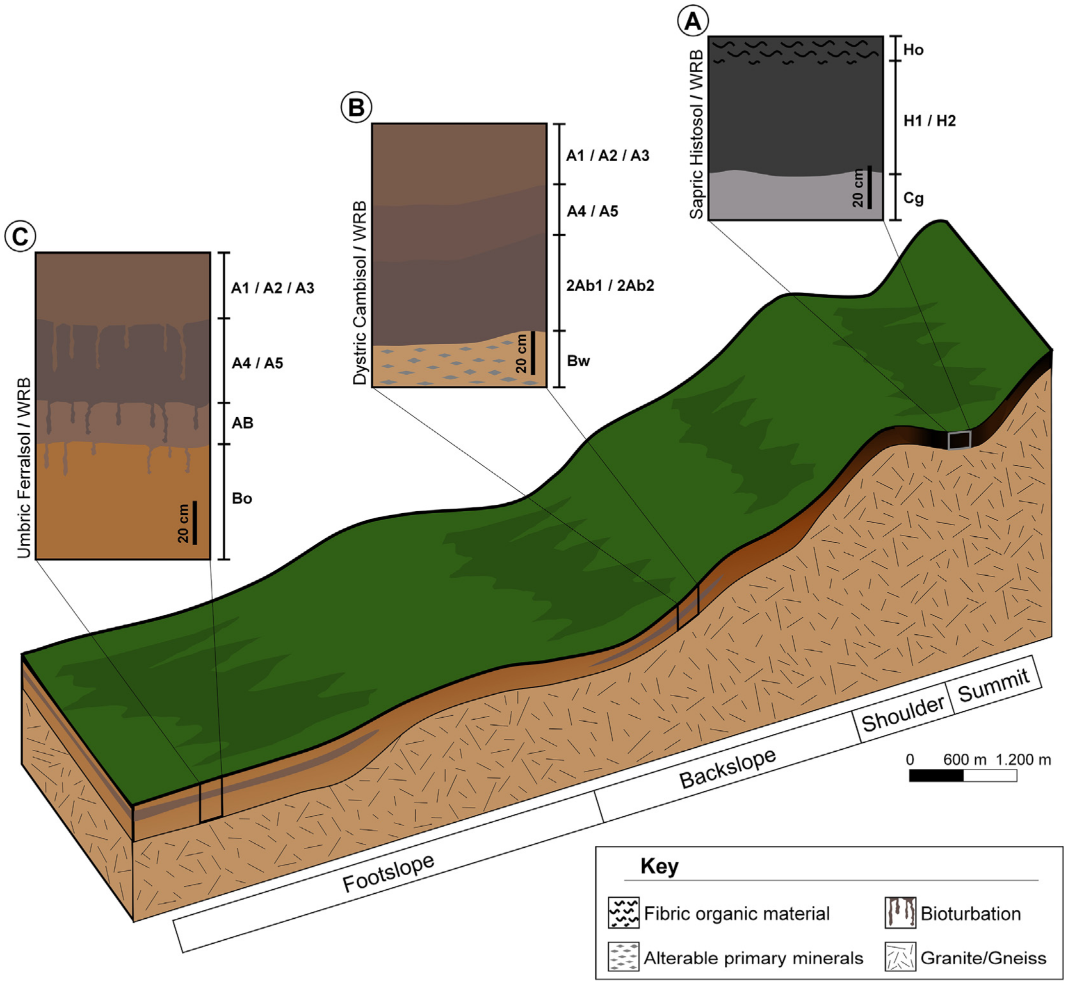

Fig. 2. Hillslope profile position of the study soil profiles in upper montane section of Mantiqueira Range, Espírito Santo State, SE region of Brazil.

PERL'X3 automated glass bead casting machine and Herzog semi-automatic pellet press. The pellets were then analyzed using a Philips Magix Pro XRF wavelength dispersive X-ray fluorescence (WDXRF) spectrometer (PW-2440), with Rh anode X-ray generator operating at 4 kW (Hallett and Kyle, 1993), and four 200 and 750µ aluminum, 300µ bronze and lead filters. The spectrometer included a Philips PW2540VRC sample changer with five sample trays with 12 positions, allowing 60 samples to be analyzed per run. Ki and Kr indices were calculated from the results of sulfuric attack and X-ray fluorescence, according to the following equations:

$$\mathrm{Ki} = \frac{1.70 \times \%\mathrm{SiO_2}}{\%\mathrm{Al_2O_3}} \qquad \mathrm{Kr} = \frac{1.70 \times \%\mathrm{SiO_2}}{\%\mathrm{Al_2O_3} + (0.64 \times \%\mathrm{Fe_2O_3})}$$

2.5. *Lithological discontinuities indicators (LDs)*

To detect possible lithological discontinuities, the uniformity value (UV) was calculated (Tsai and Chen, 2000; Schaetzl, 1998). For this, the sand fraction was separated into five sub-fractions by mechanical sieving, according to the United States Department of Agriculture (USDA) classification (USDA, 1975): silt (0.002–0.05 mm), very fine sand (VFS) (0.05–0.10 mm), fine sand (FS) (0.10–0.25 mm), medium sand (MS) (0.25–0.50 mm), coarse sand (CS) (0.5–1.0 mm) and very coarse sand (VCS) (1–2 mm). The UV was then determined using the following equation.

$$\mathrm{UV} = \frac{[(\%\mathrm{silt} - \%\mathrm{VFS})/(\%\mathrm{sand} - \%\mathrm{VFS})]_{\mathrm{in\ the\ upper\ horizon}}}{[(\%\mathrm{silt} - \%\mathrm{VFS})/(\%\mathrm{sand} - \mathrm{VFS})]_{\mathrm{in\ the\ lower\ horizon}}}$$

The ratio of total concentrations of titanium (Ti) to zirconium (Zr) was also used to identify possible discontinuities of the parent material. These elements are considered to have poor mobility due to the high stability of their naturally occurring forms in the soil environment (Milnes and Fitzpatrick, 1989) and their highly limited solubility (Taboada et al., 2006). Therefore, they have been used in various soil genesis studies to infer lithological discontinuities.

2.6. *Isotopic composition ($\delta^{13}C$) and ^{14}C dating*

Stable isotopes were analyzed in samples collected at 10-cm intervals, from the top to the bottom of the soil profile. The isotope ratio was quantified by an isotope ratio mass spectrometer (IRMS) (Delta V Advantage) coupled to an IRMS elemental analyzer (Flash EA 2000), both from Thermo Fisher Scientific (Bremen, Germany), at the Carbon and Nitrogen Biotransformation Research Laboratory (LABCEN) of the Federal University of Santa Maria, Rio Grande do Sul, Brazil. Elemental composition (SOC) was expressed as dry weight percentage, and the isotopic composition (δ^{13}C) was measured in relation to the Vienna Pee Dee Belemnite (VPDB) standard, and expressed as parts per thousand (‰, ppt) with a 0.2‰ standard deviation (Boutton et al., 1998), according to the following equation:

$$\delta_{\mathrm{sample}}\ (\text{‰}) = \left(\frac{\mathrm{R_{sample}}}{\mathrm{R_{PDB}}}\right)\left(\frac{\mathrm{R_{sample}} - \mathrm{R_{standard}}}{\mathrm{R_{standard}}}\right) \times 1000$$

where R = ^{13}C/^{12}C for the isotopic ratio of carbon.

Due to a lack of coal fragments, ^{14}C dating was performed on the humin fraction of soil organic matter (SOM), which corresponds to the

Table 1
Morphological characteristics of soil profiles from the upper montane section of Mantiqueira Range, Espírito Santo State, SE region of Brazil.

Hor[(1)]	Depth	Munsell		Soil structure [(2)]	Consistence(moist) [(3)]	Transition	Texture class
	cm	moist	dry				
P1 Sapric Histosol (WRB)							
Ho	0–18	10YR 2/1	10YR 3/2	mo., m./c, gr.	v. friable	smooth/diffuse	Organic
H1	18–40	10YR 1/1	10YR 3/1	mo., m., gr.	v. friable	smooth/diffuse	Organic
H2	40–76	10YR 4/1	10YR 3/1	mo., m., gr.	v. friable	smooth/abrupt	Organic
Cg	76–85	10YR 4/1	10YR 6/3	mac.	firm	–	Sandy loam
P2 Dystric Cambisol (WRB)							
A1	0–10	10YR 3/4	10YR 5/2	mo., m., gr.	v. friable	smooth/diffuse	Sandy loam
A2	10–19	10YR 3/4	10YR 5/2	mo., m., gr.	v. friable	smooth/diffuse	Sandy loam
A3	19–32	10YR 3/4	10YR 4/6	mo., f./m., gr.	v. friable	smooth/diffuse	Sandy clay loam
A4	32–47	10YR 3/4	10YR 4/6	mo., f., sbk.	v. friable	smooth/diffuse	Sandy clay loam
A5	47–66	10YR 3/4	10YR 5/2	mo., m., sbk.	v. friable	smooth/clear	Sandy clay loam
2Ab1	66–89	10YR 3/3	10YR 4/3	st., m./c., sbk.	friable	smooth/diffuse	Sandy clay loam
2Ab2	89–110	10YR 3/3	10YR 5/3	mo., f./m., sbk.	friable	smooth/clear	Sandy clay loam
2Bw	110–134 +	10YR 4/4	10YR 5/4	we., f./m., abk.	v. friable	–	Sandy loam
P3 Umbric Ferralsol (WRB)							
A1	0–18	10YR 4/2	10YR 5/3	we., vf./f., gr.	v. friable	smooth/diffuse	Sandy loam
A2	18–35	10YR 4/2	10YR 4/3	mo., m./c., gr.	friable	smooth/diffuse	Sandy loam
A3	35–48	10YR 4/2	10YR 5/3	we., f./m., gr.	friable	smooth/clear	Sandy clay loam
A4	48–66	10YR 3/1	10YR 3/3	st., m/c., gr.	friable	smooth/diffuse	Sandy clay loam
A5	66–86	10YR 3/2	10YR 3/3	st., m/c., gr.	friable	smooth/diffuse	Sandy clay loam
AB	86–104	10YR 4/2	10YR 5/2	mo., f./m., gr.	v. friable	smooth/clear	Sandy clay loam
Bo	104–141 +	10YR 4/4	10YR 5/6	mo., f., sbk.	v. friable	–	Sandy clay loam

[(1)] Hor = horizon.
[(2)] Grade: we = weak, mo = moderate, st = strong; Size: vf = very fine, f = fine; m = medium, c = coarse; Type: gr = granular, abk = angular blocky, sbk = subangular blocky.
[(3)] v. friable = very friable.

average residence time of the SOM (Pessenda, 1996).

The deepest organic horizons and/or mineral horizons whose organic matter concentrations were high enough for humin separation (SOC $\geq$ 40 g C kg^{-1}) were selected. The samples were collected carefully to avoid contact with organic substances or with tools and collectors possibly contaminated with organic waste. The chemical pretreatment with Acid-Base-Acid (ABA) aimed the humin isolation. The first treatment with acid used HCl 0.5 M at 80 °C, leaving the suspension resting for 4 h, for removal of light fractions of SOM such as the fulvic acids. After the removal of the supernatant, $Na_4P_2O_7$ and NaOH 0.1 M were added and the suspension left for 12 h for solubilization of humic acids, repeating the procedure up to a maximum of three times. The last treatment used HCl 3 M and heating, between 90 °C and 100 °C for 12 h; for removal of organic residues and contamination by atmospheric CO_2 (Pessenda, 1996). After the separation, samples were sent to the Center for Applied Isotope Studies (CAIS), University of Georgia, USA, for analyses using the Accelerator Mass Spectrometry (AMS). The dating results were expressed as calibrated years Before Present (cal, yr BP, 2σ; Reimer et al., 2013).

2.7. Phytolith analysis

Phytoliths were extracted from samples collected in organic horizons, by calcination in a muffle furnace, according to procedures modified by Piperno (2006). In samples collected from mineral horizons, phytoliths were extracted according to Method 2, described in Calegari et al. (2013b). The morphotypes were identified from slides prepared with the extraction fraction and observed at 400× magnification, under a Zeiss Axioskop 40 optical microscope, at the Soil Genesis and Classification Laboratory (UFRRJ). In each sample, at least 200 phytoliths with taxonomic and/or environmental significance were counted and identified, according to the International Code for Phytolith Nomenclature – ICPN (Neumann et al., 2019).

The phytoliths were grouped, based on the morphological patterns of the source plants, into: panicoid (bilobate and cross) (Bremond et al., 2005; Twiss, 1992), pooid (rondel and trapeziform) (Twiss, 1992), chloridoid (saddle) (Twiss, 1992), bambusooid (saddle collapsed), Σ Poaceae (morphotypes produced exclusively by grasses, including those with no taxonomic significance), Σ Eudicots (block, globular psilate, and globular rugose) (Bremond et al., 2005; Piperno, 2006), Arecaceae (globular echinate) (Alexandre et al., 1999; Piperno, 2006; Barboni et al., 2007) and Cyperaceae (papillate) (Piperno, 2006). Phytolith indices, including aridity index (Iph) (Twiss, 1992), climate index (Ic) (Twiss, 1992), tree cover index (Dicot phytoliths: sum of all Poaceae phytoliths; D/P) (Alexandre et al., 1997), and bulliform index (Bi%) (Bremond et al., 2005), were calculated from the identified assemblages for climatic interpretation. In order to compare the samples and interpret the pedogenic processes, phytolith concentration was determined, according to (Albert and Weiner, 2001).

Tree Cover Index (D/P Index) (Alexandre et al., 1997)

$$D/P = \frac{(\text{Globular granulate} + \text{Globular psilate} + \text{Globular oblong})}{(\text{Bilobate} + \text{Polylobate} + \text{Cross} + \text{Rondel} + \text{Trapeziform} + \text{Saddle} + \text{Bulliform} + \text{Acicular} \cdots)}$$

Climate Index (Ic) (Twiss, 1992)

$$IC\% = \left(\frac{\text{Rondel} + \text{Trapeziform (short cell and polylobate)}}{\text{Rondel} + \text{Trapeziform (short cell and polylobate)} + \text{Saddle} + \text{Cross} + \text{Bilobate short cell}}\right) \times 100$$

Aridity Index (Iph) (Twiss, 1992)

$$Iph\% = \left(\frac{\text{Saddle}}{\text{Saddle} + \text{Cross} + \text{Bilobate short cell}}\right) \times 100$$

Bulliform Index (Bi) (Delhon, 2005)

$$Bi = \frac{\text{Bulliform cells (Bulliform cuneiform} + \text{Bulliform paralelepipedal)}}{\text{Saddle} + \text{Cross} + \text{Bilobate short cell} + \text{Polylobate} + \text{Trapeziform (short cell, sinuate, polylobate)} + \text{Rondel} + \text{Bulliform}}$$

2.8. Statistical analyses

The results from the phytolith tests were assessed by multivariate statistical analyses. In each profile, similarity-clustering analyses (total sum of squares method) were performed to define phytolith zones, in TiliaGraph and CONISS (Grimm, 1987). For paleoclimatic interpretation of landscape changes, the results were evaluated by principal component analysis (PCA) in correlation mode with transposed data matrices, using the C2 software (Juggins, 2007). In this analysis, the amount of taphonomized phytoliths was also included as a variable. This type of analysis allows an ecological interpretation of phytolith data by summarizing the composition of the sample assemblages based on covariance.

3. Results

3.1. Soil morphology and general characteristics

Morphological characteristics are showed in Table 1. The soil profiles were classified according to the World Reference Base for Soil Resources (IUSS Working Group WRB, 2015) as: P1 – Sapric Histosol, it has a histic horizon under current poorly aerated conditions, but with a high degree of SOM decomposition (sapric); P2 – Dystric Cambisol, it has a cambic horizon, indicating weak pedogenesis but is better drainage than P1; and P3 – Umbric Ferralsol, the most weathered and genetically developed profile, with a ferralic subsurface horizon and a thick and dark umbric horizon, with high SOM content.

The soils in the study showed a high SOM content, due to the relatively cold climate conditions, typical of highland environments of southeastern region of Brazil. The particle size fractions varied between horizons in the profiles (Table 2), providing key information regarding the environmental characteristics and pedogenic processes. In mineral horizons, the textural classes, defined by particle size analysis, ranged from loam to sandy loam, which matches the characteristics of the parent material of the studied soils, i.e., granitic and gneiss rocks. In general, soils derived from felsic rocks, such as granite (rich in feldspar and quartz), have a coarse texture and high permeability, conditions that, especially under humid climates, favor the weathering of minerals and leaching of soluble elements. The P2 profile, in the backslope, showed the highest variations in particle size fractions along the profile. Between the A5 (47–66 cm) and 2Ab1 (66–89 cm) sub horizons, the values of the coarse and fine sand fractions varied from 157 g kg^{-1} to 395 g kg^{-1} and from 238 g kg^{-1} to 380 g kg^{-1}, respectively, further indicating a lithological discontinuity. The clay and silt values were more homogeneous throughout the profile. In the other profiles (P1 and P3), the sand fractions showed a similar pattern with depth, with no significant variations, indicating uniformity between horizons.

The soils showed strongly acidic reactions, with pH values ranging from 4.3 to 5.8 (Table 2). Higher acidity was observed in organic horizons (P1), reflecting the effect of organic material, which provides a high content of H^+ to the sorption complex. The chemical analysis of soils revealed very low nutrient (Ca^{2+}, Mg^{2+}, K^+ and Na^+) concentrations in the profiles, reflecting the parent material characteristics, which consisted of acid igneous and derived metamorphic rocks, and the tropical soil formation environment (climate and vegetation). The

Table 3
Soil organic carbon (SOC), soil total nitrogen (STN) and C:N ratios of soil profiles from the upper montane section of Mantiqueira Range, Espírito Santo State, SE region of Brazil.

Hor[(1)]	Depth (cm)	SOC	STN	C:N
		$g.kg^{-1}$		
P1 Sapric Histosol (WRB)				
Ho	0–18	87.7	3.9	23
H1	18–40	92.6	3.6	26
H2	40–76	122.0	7.6	16
Cg	76–85	44.2	2.5	18
P2 Dystric Cambisol (WRB)				
A1	0–10	75.6	4.2	18
A2	10–19	69.1	3.9	18
A3	19–32	54.3	3.6	15
A4	32–47	62.7	3.6	18
A5	47–66	56.5	2.9	20
2Ab1	66–89	54.2	2.3	23
2Ab2	89–110	62.5	2.2	28
2Bw	110–134+	21.7	1.4	15
P3 Umbric Ferralsol (WRB)				
A1	0–18	50.0	2.9	17
A2	18–35	55.8	2.4	23
A3	35–48	55.6	2.3	24
A4	48–66	51.5	2.2	23
A5	66–86	41.4	1.9	22
AB	86–104	30.4	1.5	20
Bo	104–141+	18.9	1.1	18

Table 2
Physical and chemical characteristics of soil profiles from the upper montane section of Mantiqueira Range, Espírito Santo State, SE region of Brazil.

	CS	FS	Silt	Clay	pH	S	Al^{3+}	H^+	T	V	m	P	SOC
	$g.kg^{-1}$				H_2O	$cmol_c.kg^{-1}$				%		$mg.kg^{-1}$	$g.kg^{-1}$
P1 Sapric Histosol (WRB)													
Ho	281	289	191	239	4.6	0.4	3.3	23.1	26.8	2	89	2	87.7
H1	253	289	187	271	4.3	0.4	3.1	24.2	27.7	1	89	1	92.6
H2	277	267	174	282	4.6	0.5	2.7	19.7	22.8	2	85	2	122.0
Cg	356	242	236	166	4.8	0.3	1.6	12.3	14.2	2	83	0	44.2
P2 Dystric Cambisol (WRB)													
A1	410	339	134	117	5.5	1.5	1.6	5.7	8.7	17	52	2	75.6
A2	380	264	145	211	4.9	1.1	2.3	5.0	8.3	13	69	2	69.1
A3	360	275	159	206	5.3	1.0	1.9	4.4	7.3	14	65	1	54.3
A4	370	278	148	204	5.3	0.7	1.6	3.2	5.5	13	69	1	62.7
A5	395	238	165	202	5.4	0.5	1.9	4.6	7.1	8	78	1	56.5
2Ab1	157	380	198	265	5.4	0.5	2.2	5.3	8.0	7	81	2	54.2
2Ab2	215	307	224	254	5.2	0.3	1.9	5.2	7.4	5	84	1	62.5
2Bw	251	284	287	178	5.1	0.4	1.3	4.3	5.9	6	78	0	21.7
P3 Umbric Ferralsol (WRB)													
A1	464	294	85	157	5.1	0.7	1.2	3.4	5.3	13	64	2	50.0
A2	442	294	75	189	5.1	1.3	1.4	4.6	7.3	18	52	2	55.8
A3	415	274	89	222	5.2	0.7	1.6	4.6	6.9	11	69	1	55.6
A4	382	258	92	268	5.8	1.5	1.8	5.2	8.5	18	54	2	51.5
A5	328	278	117	277	5.0	1.1	1.6	4.8	7.5	15	59	2	41.4
AB	372	227	103	298	4.9	0.5	1.3	4.6	6.4	8	71	1	30.4
Bo	384	218	119	279	5.0	0.3	1.0	3.7	4.9	5	79	1	18.9

CS = coarse sand, FS = fine sand; S = sum of bases (S = Ca^{2+} + Mg^{2+} + K^+ + Na^+), T = cation exchange capacity (T = S + H^+ + Al^{3+}), V = base saturation (V = S/T *100), m = aluminum saturation (m = (100*Al^{3+})/(S + Al^{3+})).

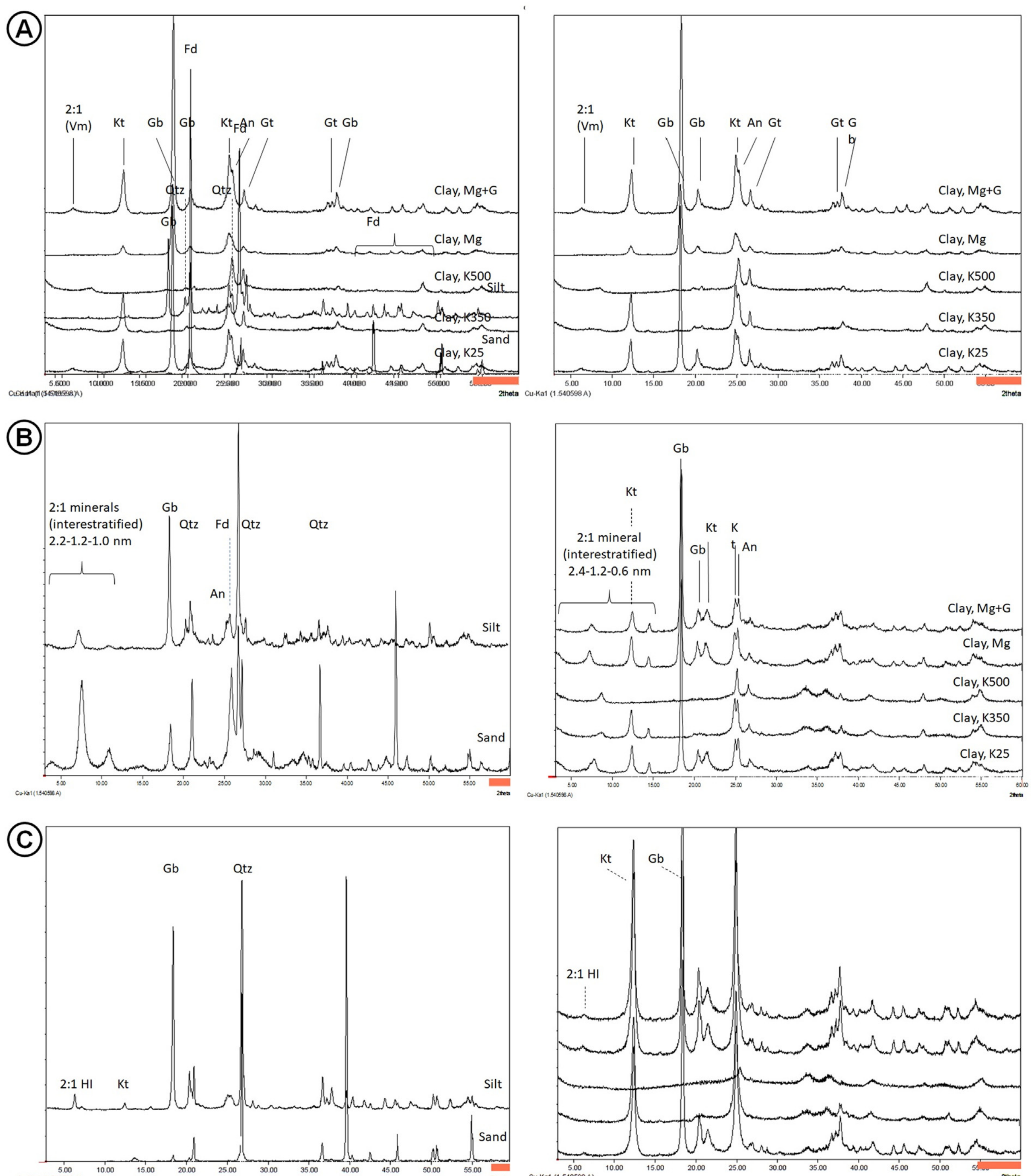

Fig. 3. XRD pattern of the sand/silt fractions (left) and clay fraction (right) of Cg horizon, profile P1 (A), Bw horizon, profile P2 (B) and Bo horizon, profile P3 (C). Gb: gibbsite; Qtz: quartz, Fd: Feldspars, Vm: vermiculite; Kt: kaolinite; Gb: gibbsite; An: anatase (A); 2:1 HI: Hydroxy interlayered 2:1 phyllosilicate.

high values of cation exchange capacity (T) is a result of the high SOM content.

The values of SOC ranged from 44.2 to 122.0 g·kg^{-1} in the profile P1, 21.7 to 69.1 g·kg^{-1} in the profile P2, and from 18.9 to 55.8 g·kg^{-1} in the profile P3 (Table 3). For the soil total nitrogen (STN), the values ranged from 2.5 to 7.6 g·kg^{-1} in the profile P1, 1.4 to 4.3 g·kg^{-1} in the profile P2, and from 1.1 to 2.9 g·kg^{-1} in the profile P3. The C/N ratio varied between 15 and 28, reflecting the different intensity of humification of the SOM in the studied soil profiles. In P1, there was a tendency to decrease the C/N values with depth (Table 3), indicating a relative enrichment of N and humification in the deeper organic horizon. In the profiles P2 and P3 the C/N ratio increased with depth, indicating that there may lixiviation of fulvic fractions.

3.2. Mineralogical characteristics

In the P1, Cg horizon, the sand fraction showed peaks of feldspar (21.14 2theta, 4.2 nm) and quartz (27 2theta, 3.33 nm) minerals. As expected, the primary minerals dominating this fraction exhibited a small full width at half height (FWHH), because of their high degree of crystallinity (Fig. 3A). This is in accordance with the granitic/gneissic nature of the soils parent material. In the silt fraction, the appearance of a sharp and strong peak of gibbsite (18.37 2theta, 4.8 nm) implies that a considerable amount of feldspar had weathered. The clay fraction

(Fig. 3A) showed a small amount of 2:1 phyllosilicate, probably a vermiculite, as the peak moved to 1.4 nm (6.48 2 theta) when it was saturated with Mg and glycerol, and back to 1.0 nm (8.64 2theta) after K saturation and heating to 550 °C. However, kaolinite (confirmed by the disappearance of its main peak at 7.2 nm, 12.58 2theta after heating to 550 °C) and gibbsite (confirmed by the disappearance of its main peak at 4.8 nm, 18.45 2theta after heating to 350 °C) were the most abundant mineral phases, as estimated by the integrated intensity of their peaks. This mineralogy is in concordance with the chemical analysis (Table 2), which shows the lowest pH and highest exchangeable Al for this horizon, compared to the B horizons of P2 and P3 profiles. This suggests that the feldspar is rapidly weathering to kaolinite and gibbsite. The 2:1 mineral mentioned previously might have been formed either from the release of silica and aluminum from the feldspar, or from the alteration of mica from the parent material. Regardless of its origin, it seems to have a short lifespan in this acidic environment, as inferred from its small amount in the soil.

The P2 profile exhibited a great contrast between the sand and silt fractions (Fig. 3B). The sand fraction showed a series of three peaks (22.7 nm, 3.9 2theta; 11.7 nm, 7.73 2theta; 8.0 nm, 11.0 2theta) indicating the possibility of interstratified 2:1 phyllosilicate, while the silt fraction showed a single peak (12.4 nm 7.12 2theta), indicating that the transformation of mica to the 2:1 phyllosilicate was complete. In addition, the peaks of feldspar exhibited a sharp decrease, while those of gibbsite and anatase increased. The weathering gap between these two fractions appeared to be wider in this profile, than in the P1 and P3 profiles. This agrees with other lithological discontinuity indicators (discussed in the following sections), which suggest a greater external input of materials in P2. In the clay fraction (Fig. 3B), the interstratified series was again observed (2.4, 1.2 and 0.6 nm, 3.65, 7.27 and 14.61 2theta). All these phases collapsed to 1.0 nm (8.82 2theta) upon heating to 550 °C with K saturation. This further supports the lithological discontinuity hypothesis, since these interstratified phases appeared only in the sand and clay fractions. Gibbsite and kaolinite were the most abundant clay minerals, and their presence was confirmed from the disappearance of their peaks by heating at 350 °C and 550 °C, respectively.

The P3 mineralogy was typical of the Ferralsols. The sand and silt fractions (Fig. 3C) showed a small amount of 2:1 hydroxy interlayered (HI) minerals, and quartz. The gibbsite was highly crystalline, which has been pointed as common in high altitude soils, and the small amount of kaolinite might be due to incomplete extraction of the clay fraction. The clay fraction showed a small amount of 2:1 HI minerals and dominance of gibbsite and kaolinite (Fig. 3C).

3.3. Ki and Kr indices and total elements

Total content of soil oxides (SiO_2, Fe_2O_3, Al_2O_3 and TiO_2) are outlined in Fig. 4. The high SiO_2 and Ki values observed in P1 indicate silica accumulation in the profile influenced by the soiĺs poor drainage. This profile was located in a concave portion of the slope and presented a histic (H) horizon formed from materials deposited under excess water conditions, for extended periods or throughout the year.

In the P2 profile, along with the evidence of lithologic discontinuity, the results revealed its polygenetic origin. The TiO_2 percentage increased from 0.98% (A5) to 2.06% (2Ab1) in the P2 profile. In soil, Ti is an element found in highly stable minerals, and is therefore used, along with other parameters, as an indicator of lithological discontinuity in the profile (Taboada et al., 2006). Other relevant parameters are the molecular ratios Ki and Kr, which also showed significant variations in this profile, indicating less weathered materials in the upper section of the profile, which corroborates the hypothesis of external material input.

The P3 profile, classified as Ferralsol, showed the greatest SiO_2 losses and a relative increase in Fe_2O_3 and Al_2O_3. These results express a highly advanced pedogenesis with marked ferralitization, resulting in intense weathering of the primary minerals and even of less resistant secondary minerals, and a high relative concentration of resistant clay minerals and/or iron and aluminum oxides and hydroxides in the clay fraction. The values of Ki and Kr > 0.75 are used in the Brazilian System of Soil Classification (Santos et al., 2018), to indicate a dominant kaolinitic composition of the clay.

3.4. Lithological discontinuities indicators (LDs)

The results of the variation in UV and Ti/Zr ratio are shown in Fig. 5. The most significant variations in these two parameters were observed in the P2 profile, which showed morphological evidence of lithological discontinuity. The UV for this profile was 0.78 in the A5/2Ab1 transition. Conversely, the Ti/Zr ratio increased from 5.5 (A5) to 15.7 (2Ab1) in the same profile. These results, together with the morphological (color, texture, structure) and chemical (organic carbon, molecular ratios) properties, corroborate the observed discontinuity pattern, which, in this case, is a result of the colluviation process. The surface horizons correspond to materials mobilized from the upper sections of the landscape, carried by gravity and deposited on the surface of an ancient soil. Colluviation is known to be involved in the thickening of humic A-horizons and that these horizons are evidence of polygenic soils (Calegari, 2008).

3.5. ^{14}C dating and isotopic composition ($\delta^{13}C$)

The dates in the three assessed profiles revealed that the humin fraction had similar ages, ranging from −2300 to −2000 cal. yr BP, corresponding to the Late Holocene (Table 4). The SOM is almost exclusively derived from groundcover, often serving as a testimony of past climatic conditions.

The results of $\delta^{13}C$ isotopic composition showed different patterns as a function of depth, with variations larger than 4‰ in almost all profiles (Fig. 6), indicating changes in the plant communities during soil formation. The application of stable carbon isotopes ($^{13}C/^{12}C$) makes it possible to differentiate groups of plants based on their photosynthetic cycle, i.e., C_3 and C_4 plants, and thus, to infer vegetation characteristics, whereas ^{14}C dating (of humin fraction) indicates the age of the records (Pessenda, 1996). The $\delta^{13}C$ values of C_3 plants range from −22.0‰ to −32.0‰ (mean = −27.0‰), and those of C_4 plants range from −9.0‰ to −17.0‰ (mean = −13‰) (Boutton et al., 1998). Thus, the $\delta^{13}C$ values of the SOM can be used to infer changes in the vegetation structure and, indirectly, in the humidity and climatic conditions of the area at the time they were incorporated into the soil.

The surface $\delta^{13}C$ values represent the current vegetation of the profiles, as described previously, consisting predominantly of C_3 plants in P1 (−23.15‰), a mixture of C_3 and C_4 plants in P2 (−20.47‰), and predominantly C_4 plants in P3 (−15.65‰). The P1 profile showed an isotopic depletion from the bottom to the top of the profile, with values ranging from −15.44‰ (−90 cm) to −23.15‰ (−10 cm), indicating a base consisting primarily of C_4 plants, most likely associated with a climate less humid or drier than the present, and the subsequent expansion of C_3 plants 2.063 cal. yr BP. The other profiles showed the same pattern of variation, marked by isotopic depletion from 110 to 80 cm (mean = −28.84‰ ± 0.72) in profile P2, and from −90 to −60 cm (mean = −28.28‰ ± 1.27) in profile P3. This variation indicates a phase dominated by C_3 plants, which most likely occupied much of the toposequence, from the footslope to the backslope, possibly due to a humid climate, from −2.229 to −2.330 cal. yr BP. From these depths, the profiles showed isotopic enrichment until the surface, reaching −19.45‰ in P2 and −15.65‰ in P3. These results indicate a mixture of C_3 and C_4 plants, as observed in the modern vegetation, which dominated both sampling sites, most likely associated with a less humid climate than that prevailing in the past.

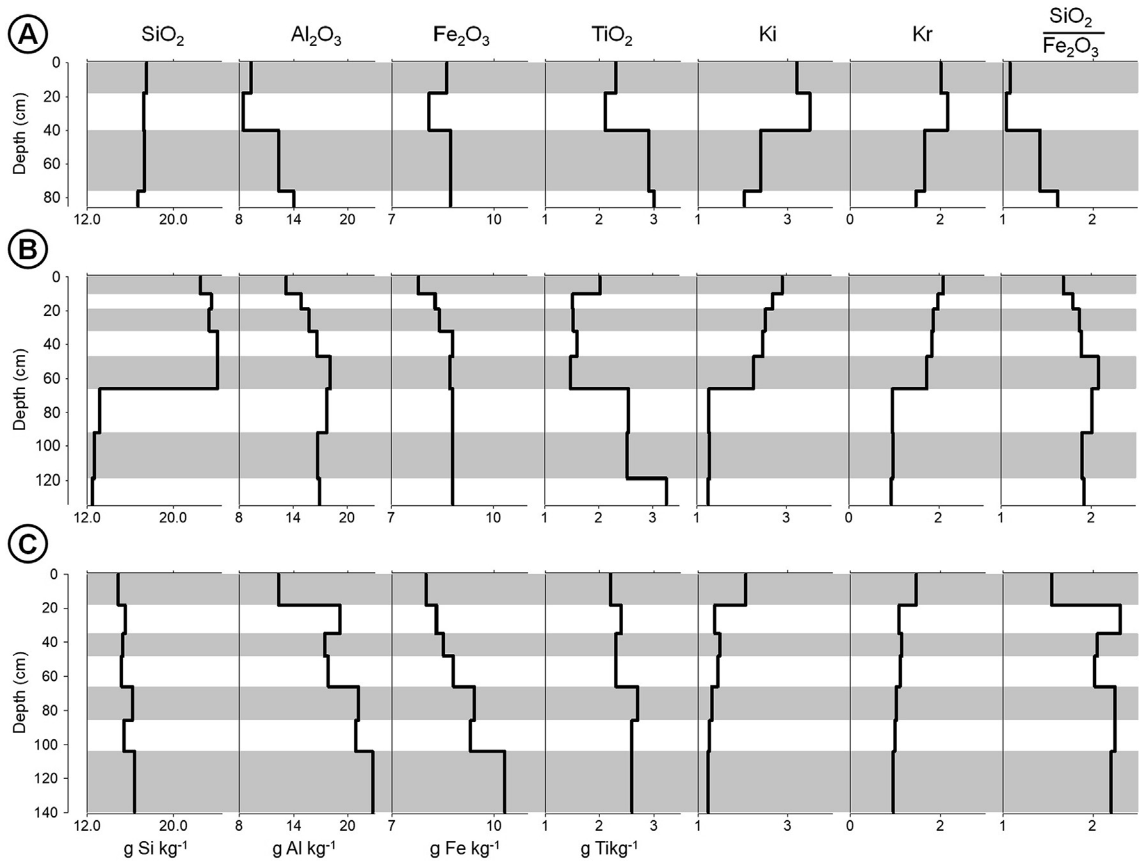

Fig. 4. Variation on depth from sulfuric attack, X-ray fluorescence and molecular ratios in the soil profiles studied in upper montane section of Mantiqueira Range, Espírito Santo State, SE region of Brazil.

3.6. Phytolith analysis

All study profiles showed a high phytolith frequency, with different patterns of variation as a function of depth along the toposequence (Fig. 7), and phytolith frequencies were always higher in surface soil horizons. Grasses (Poaceae Family) were the dominant taxon in all samples, and the subfamilies Pooideae, Panicoideae, and Chloridoideae were the most represented in phytolith assemblages. Morphotypes produced by tree and shrub species (Eudicots) were also observed, although always with a lesser percentage. Other plant groups identified with significant phytolith concentrations included the families Arecaceae and Cyperaceae.

In all profiles, the phytolith assemblages observed in the first few centimeters (0–10 cm) corresponded to the phytolithic signature of current vegetation, consisting of a mosaic of dense montane rainforest or high montane forest plants interspersed with herbaceous-shrub vegetation. At the surface, the following values of phytolith indices were observed: P1 D/P = 30%, Ic = 50%, Iph = 48% and Bi = 24%; P2 D/P = 19%, Ic = 48%, Iph = 21% and Bi = 15%; P3 D/P = 19%, Ic = 48%, Iph = 21% and Bi = 15%. The most abundant morphotypes (%) identified in the assemblages were elongated and hair cells (13–47%, mean = 31% ± 2.3), both without taxonomic significance, as they are produced by all grass subfamilies (Barboni et al., 2007). Among the morphotypes with taxonomic significance, those that stood out were rondel and trapeziform short cells (7–24%, mean = 14% ± 3.7), produced by grasses of the Pooideae subfamily, characteristic of temperate or high altitude regions in the tropics, as well as bilobate and cross morphotypes (7–20%, mean = 14% ± 2.7), typical of the Panicoideae subfamily, consisting of tall grasses of tropical zones, adapted to hot and wet climate conditions. Phytoliths produced by woody plants with tree and shrub habits accounted for 2–26% (mean = 11% ± 1.6) surface phytolith assemblages.

The hierarchical clustering identified three phytolithic zones in each profile (Fig. 5). **Zone I** corresponded to horizons with morphological features resulting from the pedogenic process of gleization in profile P1. In the profiles P2 and P3 the Zone I corresponded to the B horizon. In all profiles, the assemblages in this zone showed high concentrations of taphonomized phytoliths (mean P1 = 18% ± 2.2, P2 = 156% ± 0.2, P3 = 14% ± 1.7), indicating a longer residence time of these phytoliths in the soil. In profiles P2 and P3, this zone had the lowest values of tree cover (D/P) and climate (Ic) indices, indicating more open vegetation in a climate warmer than the current conditions, whereas the isotopic values indicate a mixture of C_3 and C_4 plants. In general, the assemblages of the samples from this cluster consist of morphotypes produced by plants more adapted to hot and dry weather conditions, as indicated by the higher values of the aridity (Iph) (mean P1 = 57% ± 0.8, P2 = 61% ± 1.7, P3 = 62% ± 2.6) and bulliform (Bi) (mean P1 = 26% ± ,2.2 P2 = 52% ± 1.9, P3 = 51% ± 5.8) indices.

Zone II corresponded to horizons with sapric organic material in P1, to buried horizons in P2, and to dark subsurface horizons in profile P3. In profile P2, the upper limit of this zone corresponded to the lithological discontinuity identified based on the UV and Ti/Zr ratio. The concentration of phytoliths also increased in this profile, indicating the presence of buried horizons. The phytolith indices showed an increased frequency of morphotypes produced by trees and shrubs (Eudicots) and by plants more adapted to cooler and wetter conditions. The mean D/P index was 21% ± 4.8 in P1, 49% ± 7.9 in P2, and 50% ± 8.7 in P3, and the Ic index was 37% ± 3.4 in P1%, 56% ± 1.6 in P2, and 56% ± 1.5 in P3. This change in vegetation type was also reflected in the isotopic values, which showed more depleted values of $\delta^{13}C$ in profiles P2 and P3. ^{14}C dating of the organic matter (humin fraction)

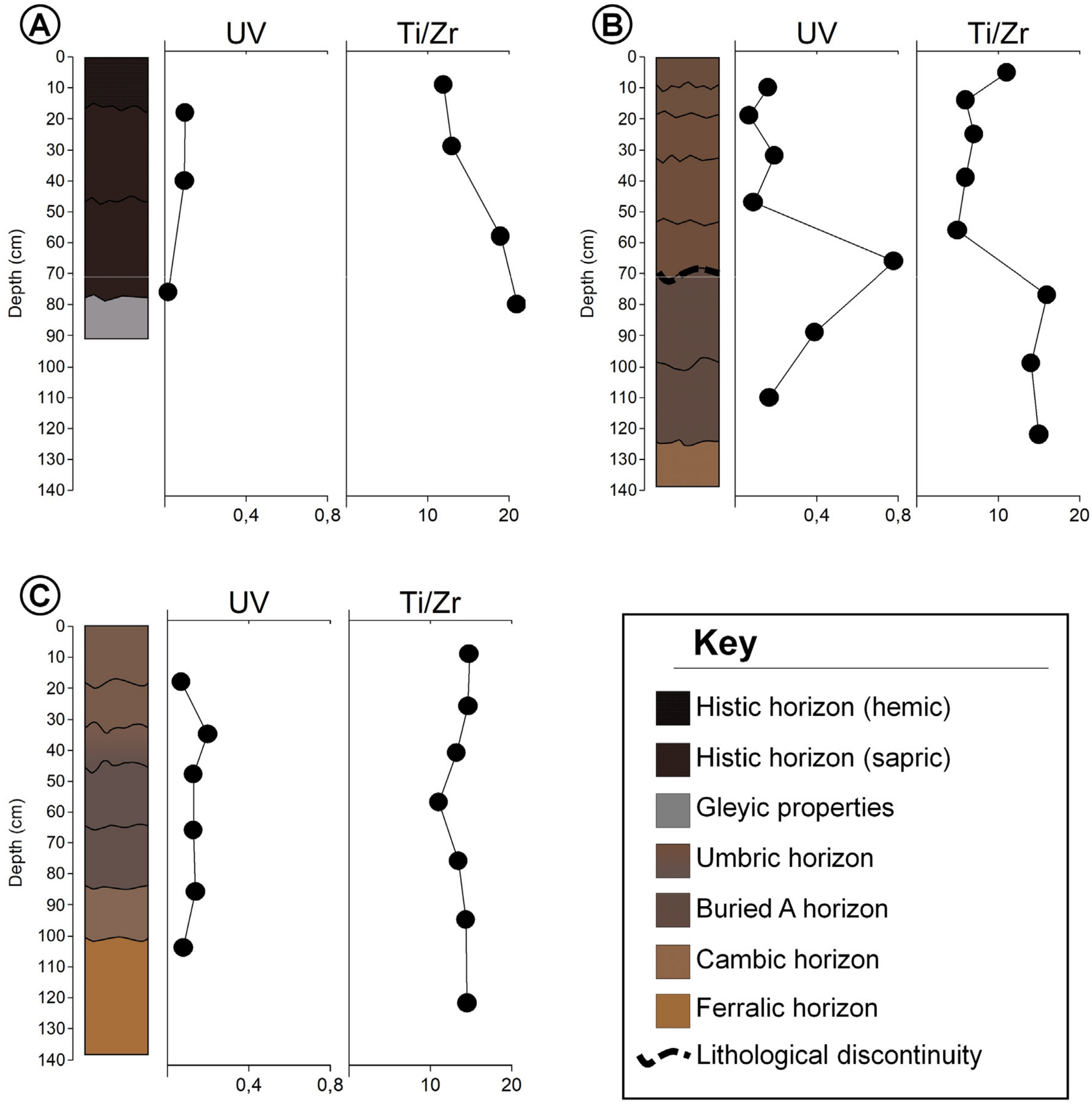

Fig. 5. Indicators of lithological discontinuities in the study profiles; UV: uniformity value; Ti/Zr: ratio between TiO_2 and ZrO_2 concentrations (X-ray fluorescence).

Table 4
Humin fraction dating by ^{14}C of soil profiles from the upper montane section of Mantiqueira Range, Espírito Santo State, SE region of Brazil.

Prof.	Hor.	Depth. (cm)	Lab Code*	2σ calibrate age BP	Medium age calibrated BP
P1	H2	40–76	UGAMS#29953	1.994–2.131	2.063
P2	2Ab2	89–110	UGAMS#29954	2.151–2.318	2.229
P3	A5	66–86	UGAMS#29955	2.306–2.352	2.330

* AMS: CAIS – Center for Applied Isotope Studies, Georgia University, USA.

suggested that this climate period would have occurred around −2.330 and −2.063 cal. yr BP. Regarding the Iph and Bi indices, all profiles showed values lower than the previous zone, with a mean Iph of 29% ± 0.8 in P1, 25% ± 1.7 in P2, and 25% ± 1.5 in P3, indicating a low frequency of plants adapted to arid conditions, and with a mean Bi of 15% ± 1.2 in P1, 21% ± 1.9 in P2, and 22% ± 2.3 in P3, reflecting soil conditions were more humid.

Zone III consisted of surface horizons. In profile P1, Zone III corresponded to the horizon with hemic organic material (with an intermediate degree of composition between fibric and sapric). In profiles P2 and P3, it corresponded to the surface A horizon. In addition, this zone corresponded to a transition phase, between the characteristics observed in the current vegetation and the dense montane rainforest/high montane forest plants interspersed with herbaceous-shrub vegetation. In the upper section of the slope, the records in the P1 profile suggest colder environment conditions (mean Ic = 52% ± 1.8) and denser tree vegetation (mean D/P = 31% ± 1.5). In profiles P2 and P3, positioned in the backslope and footslope, the phytolith data indicated the presence of less dense tree vegetation (mean D/P = 27% ± 5.4 in P2 and 27% ± 5.9 in P3) and warmer climate conditions than in the previous zone (mean Ic = 44% ± 3.4 in P2 and 44% ± 3.1 in P3). This difference in vegetation between the upper third and other sections of the toposequence was further confirmed by isotopic dating, with more enriched values in profiles P2 and P3, suggesting open vegetation (field) dominated by C_4 plants, in contrast to more depleted values in profile P1, which indicate a higher prevalence of C_3 plants. The indices related to humidity conditions, i.e., Iph and Bi, increased in P1 (mean Iph = 46% ± 2.3; mean Bi = 23% ± 1.5), which could be related to the genesis of the Histosols, in which the organic material accumulation occurred under hydromorphic environments with permanent or oscillating water table throughout the year.

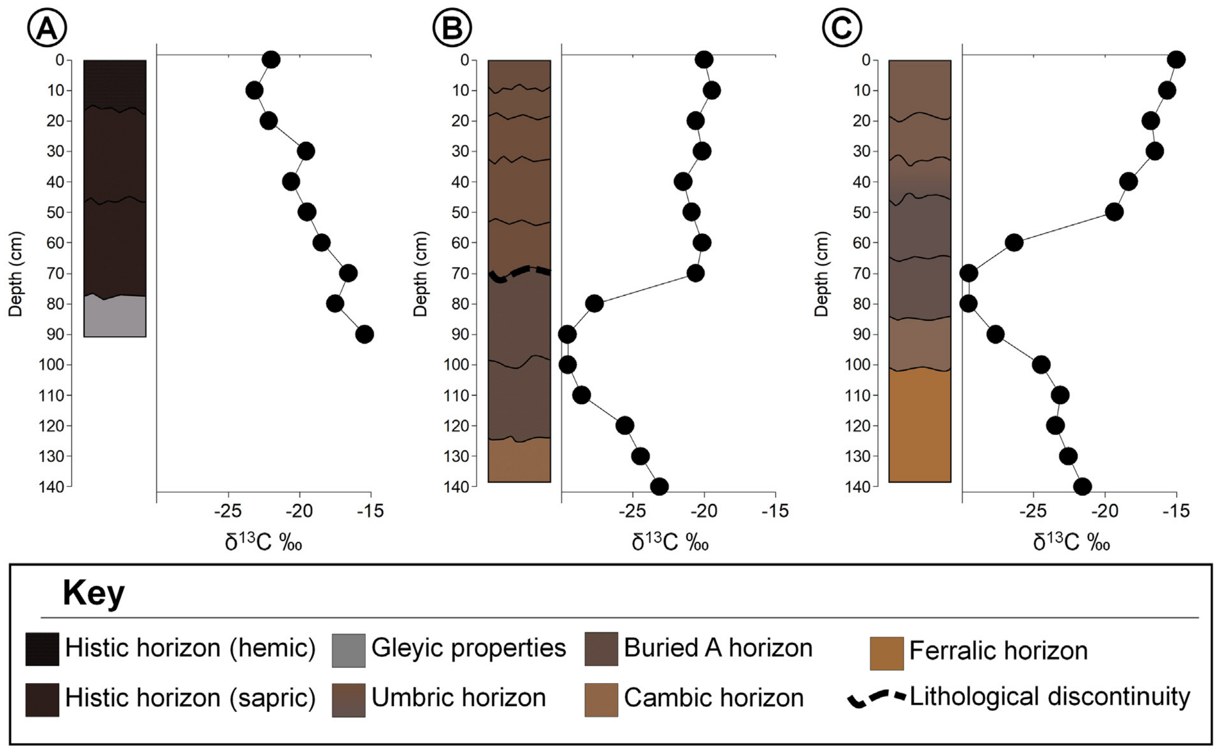

Fig. 6. Variation curves of isotopic values ($\delta^{13}C$) in the soil profiles studied in upper montane environments of Mantiqueira Range, Espírito Santo State, SE Brazil.

4. Discussion

4.1. Pedological processes

Significant variations in pedological cover highlight the relationship of the profile properties with the dynamics of the soil forming factors. Dynamic soil development is used in the sense of Johnson and Watson-Stegner (1987), according to which most soils are polygenetic and impacted by progressive (in situ soil development and incorporation of particles) and regressive (domination of removals by erosion and mass wasting) pathways during their development (Nehren et al., 2016).

The genesis of the Histosol (P1) is associated with the poor drainage environment resulting from specific conditions of relief and the influence of the parent material, consisting mainly of alteration of crystalline rocks (primarily granites and gneisses), which will affect the shape of slopes, valleys and depressions. The structural pattern of these weathering-resistant rocks hinders free drainage, thereby controlling the distribution of Histosols in the area. Similar pattern was observed in peatlands studied in the tropical highlands of Minas Gerais State, southeastern region of Brazil (Campos et al., 2017; Horak-Terra et al., 2014). In these conditions, the deposition of organic residues normally starts with the terrestrialization process, forming a peat deposit, which, in turn, is the main parent material of Histosols (Buol et al., 2011; Kroetsch et al., 2011). This is followed by the paludification process, which involves colonization of the poorly drained lands by plants, and the differentiation of organic deposits in soil horizons, with properties determined by pedogenesis processes in which the soil organic matter plays a major role.

The surface inclination (8%) and the convex shape favored the initial erosion processes leading to the formation of the Cambisol (P2) in the backslope section of the toposequence. P2 morphology is marked by the presence of a buried soil, covered by younger colluvial sediments from erosion of upper sections of the toposequence, and the profile is at an early (incipient) stage of pedogenesis. Formation of soils in tropical environments are marked by intense chemical weathering and variation of phases of erosion–deposition of materials, and the parent materials of most Brazilian soils are considered to be constituted of old and highly weathered sediments, wherein pedogenesis “welded” the soil horizons formed during different ages/periods (Ruhe and Olson, 1980). In addition to soil classification and land management implications, buried soils and genetic horizons may contain records of past environments, which are important for paleoclimatic studies.

The Ferralsol (P3), in the footslope position, is highly weathered and strongly leached, with a clay mineralogy essentially made up of gibbsite and kaolinite. The most weathered tropical soils are subjected to cumulative, long-term ferralitization, and are formed from pre-weathered materials (Schaefer, 2001). Colluvial deposition and bioturbation are common, transporting and welding soil materials, which complicates field recognition of boundaries between soils horizons and parent materials (Ruhe and Olson, 1980). In addition, low temperatures, high Al^{3+} levels and very low nutrient contents reduce microbial activity and constrain organic matter mineralization, enhancing soil carbon sink (Simas et al., 2005).

The low natural fertility in the studied profiles is related to nutrient losses resulting from the high precipitation rates and moisture, which favor weathering and leaching, plus the acidic character of the parent material (granites and gneisses). Clay minerals (1:1), Fe and Al oxides, hydroxides and oxyhydroxides with low CEC predominate in most soils of Brazil (Kämpf et al., 2012). These conditions, however, did not restrict the establishment and growth of dense Atlantic Forest vegetation, similarly to those observed by Simas et al. (2005) studying soil profiles from one of the uppermost areas of the Mantiqueira Highlands (Minas Gerais State, southeastern Brazil). Low nutrient content and high acidity of the soil help to reduce decomposition rates of organic residues, allowing them to accumulate under humid and cold conditions, such as in the upper mountainous regions of Mantiqueira Range. On the other hand, the reactions of the functional groups of SOM are the chemical basis of the soiĺs fertility, i.e., the ability to retain bases depends on the dissociation of functional groups from SOM.

The great diversity in soil attributes along the toposequence shows that the forming factors promote a wide variety of processes, as local conditions vary between sites. Landscape position is a critical factor

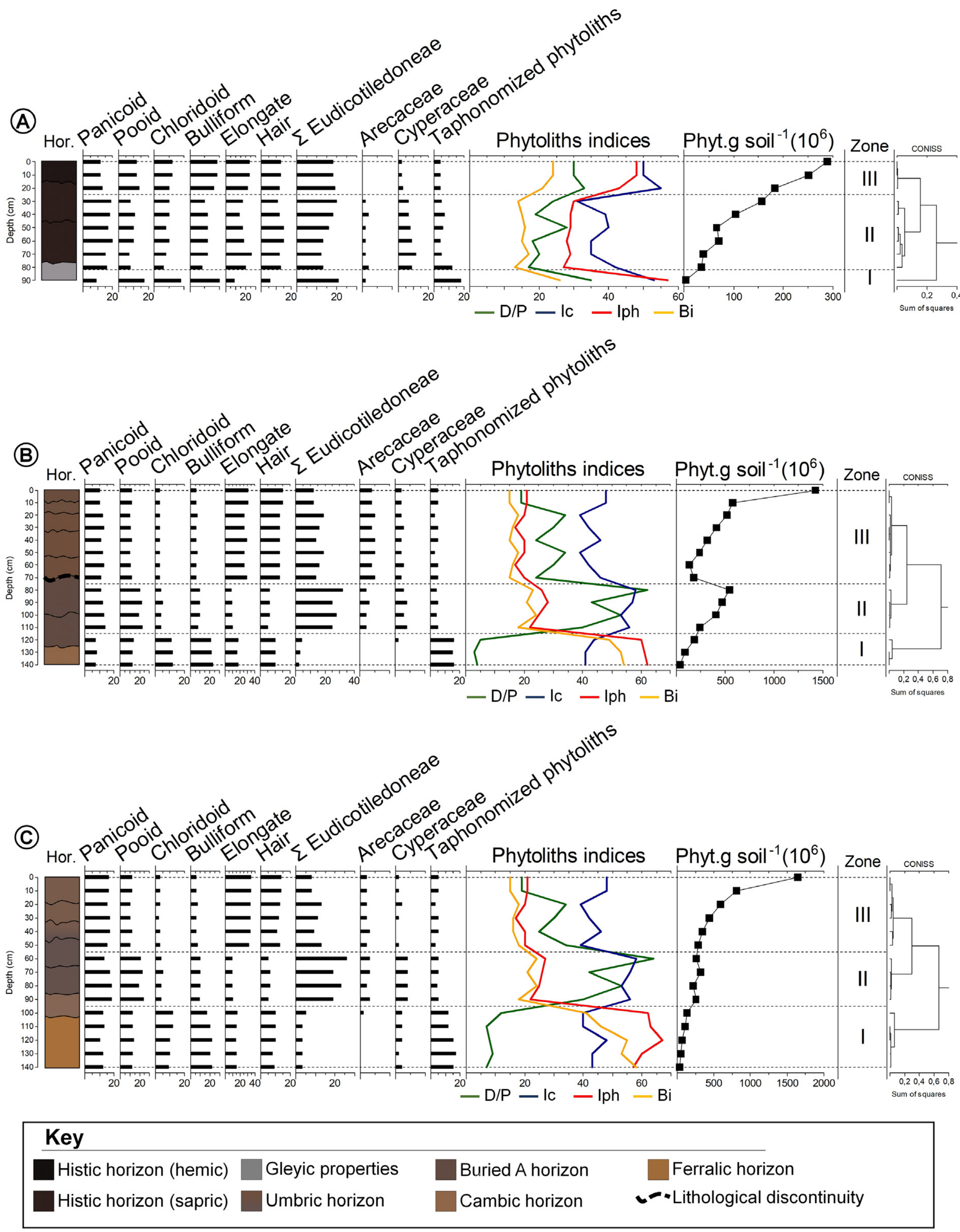

Fig. 7. Phytolithic diagrams of the soil profiles studied in upper montane section of Mantiqueira Range, Espírito Santo State, SE region of Brazil. (A) Profile P1, (B) Profile P2, and (C) Profile P3.

influencing many soil properties, like solum depth and degree of chemical weathering, including those of highly weathered soils, which tend to have a high degree of homogeneity (Curi and Franzmeier, 1984; Anjos et al., 1998).

4.2. Environmental interpretation

The graphic with the PCA results explained 81.5% of the total variance with two principal components (Fig. 8). PC1 (which represents the climate temperature) explained 46.9% of the total variance, and was characterized by globular, block, pooid, papillate, globular echinate, hair cells and elongated morphotypes in its positive quadrant, and

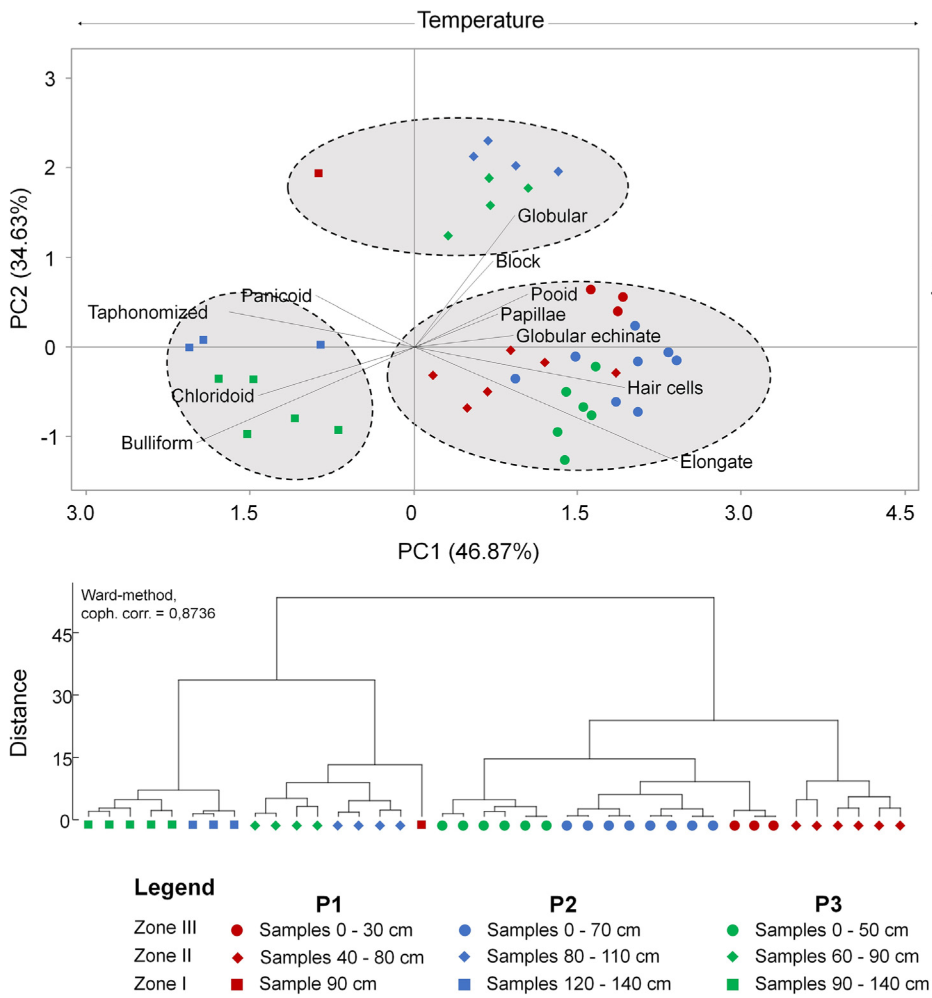

Fig. 8. Principal component analysis and hierarchical clustering in samples collected from the soil profiles studied in upper montane section of Mantiqueira Range, Espírito Santo State, SE region of Brazil.

by panicoid, chloridoid, bulliform and taphonomized morphotypes in its negative quadrant. Thus, positive PC1 values in this toposequence represent colder climate conditions, indicated by the Cyperaceae and Pooid morphotypes, which are related to cold and wet climate (Piperno, 2006). In turn, negative PC1 values indicate reduced tree cover and warmer climate conditions, with chloridoid and bulliform morphotypes, which are related to hot and dry climate conditions.

The PC2 (which represents humidity) explained 34.63% of the total variance, and was represented in the positive quadrant by globular, block, panicoid, pooid, papillate, globular echinate and taphonomized morphotypes. In the negative quadrant, this component was represented by chloridoid morphotypes, in addition to those without taxonomic significance, namely elongated, hair and bulliform morphotypes. Thus, PC2 indicates the humidity conditions of the area, with positive values representing more humid conditions and negative values representing drier conditions, as evident from the predominantly herbaceous vegetation, with few tree components.

Hierarchical clustering combined with ^{14}C dating made it possible to establish a pedochronostratigraphic correlation (Fig. 9), and to identify three environmental moments in the studied toposequence, which are as follows:

Phase I (~before −2,330 cal yr BP) was recorded in the bottom of profiles P2 and P3, and corresponds to a drier and hotter period than the current climate, with vegetation predominantly consisting of C_4 grasses (indicating conditions of lower humidity), and plants adapted to hot and dry climate conditions. At this environmental moment, mechanical morphogenesis would predominate due to sparse but torrential rainfall and sparse vegetation. Landscapes with sparse vegetation and drier climate conditions have been reported in various paleoclimatic studies conducted in southeastern Brazil (e.g. Behling, 1995; Behling and Lichte, 1997; Behling and Safford, 2010). Since the Early Quaternary, the Brazilian landscape, which has evolved under essentially tropical conditions since the Cretaceous, has suffered the consequences of global cooling (Schaefer, 2013). During glaciation in the northern hemisphere, which occurred until the Late Pleistocene, arid or semi-acid conditions developed in tropical regions. This environmental moment can be a record of this conditions, as expressed by the values of Iph (> 30%) and Bi (> 40%) indices. Although, high Bi index values may be related partly to highest resistance of the bulliform morphotypes in the soil (Calegari et al., 2013a), their occurrence together with Chloridoideae morphotypes confirmed the conditions of lower humidity. According to Messager et al. (2010), bulliform phytoliths are good indicators of water stress in grasses.

Another key result related to this climate period is the high frequency of taphonomized phytoliths. Physical weathering dominates over chemical weathering in environments with low water availability. When vegetation is sparse, soil material is highly exposed to hydric erosion associated with torrential water flows, resulting in accelerated hillside evolution and valley clogging, i.e., morphogenesis predominates pedogenesis. In addition to longer soil residence time, the high concentration of taphonomized phytoliths (broken and corroded, among others) may be related to erosion transport during this period.

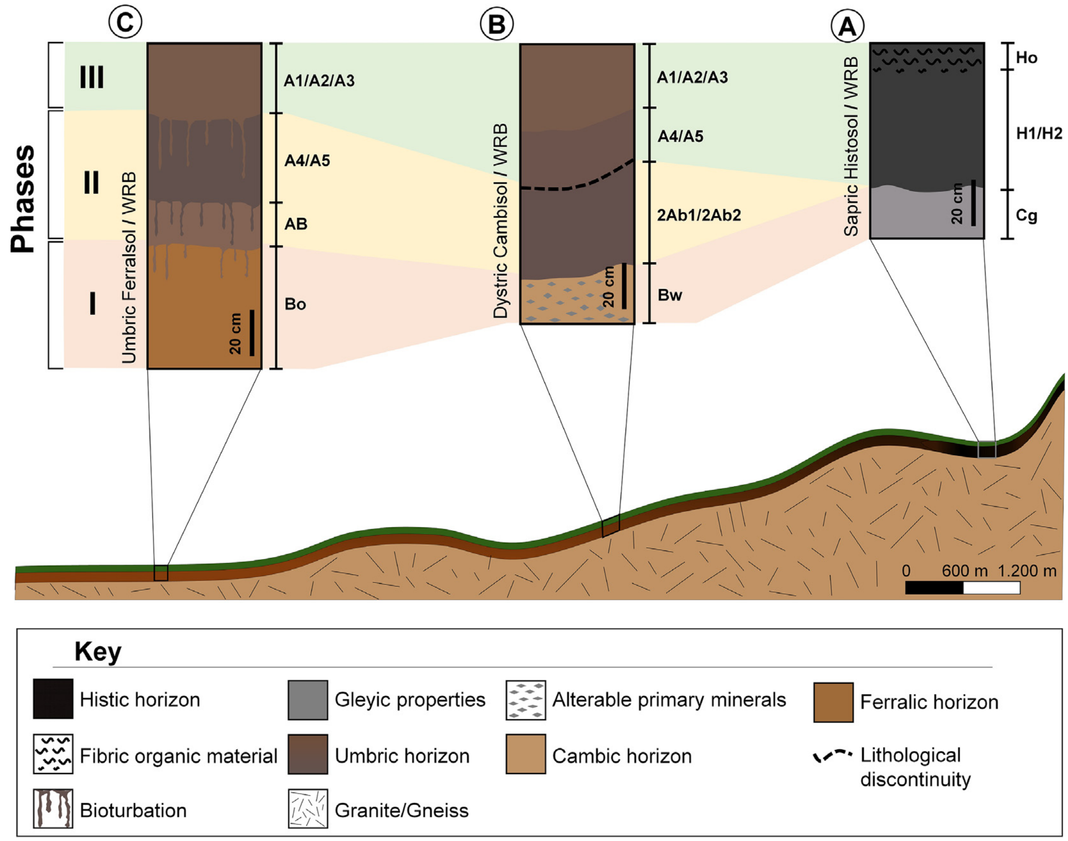

Fig. 9. Pedochronostratigraphic correlation between soil profiles studied in upper montane section of Mantiqueira Range, Espírito Santo State, SE region of Brazil.

Phytoliths are highly resistant to physical and chemical processes in sediments, and the preservation of these bioindices largely depends on the physical and chemical characteristics of the depositional environment (Piperno, 2006).

Phase II (−2330/−2063 cal. yr BP) corresponds to zone I in P1, and zone II in P2 and P3. This period corresponds to a period of more humid and colder climate than the current conditions, indicated by high D/P (> 40%) and Ic (> 55%) values. The isotopic signal of this period corresponds to vegetation consisting mainly of C_3 plants. The ^{14}C dating of samples from this soil depth corresponded to the Late Holocene, with ages ranging from 2063 to 2330 cal. yr BP. The concentration of phytoliths was also high, indicating a high input of organic residues to the soil during this period. These results corroborate the findings of Pereira et al. (2012) in Serra do Caparaó (ES), who reported an increase in the abundance of Cyperaceae, ferns and shrub genera Baccharis and Croton in the same geomorphological region, indicating more humid climate conditions and the forest expansion around 2.670 cal. yr BP.

This climate period would be related to the formation of buried A horizon in profile P2, showing that the landscape evolution occurs as a result of periodic or episodic erosion, rather than at a uniform rate (Anjos et al., 1998). In the P1 profile, this phase marks the beginning of SOM accumulation, with peat accumulation, demonstrating interrelationships between formation factors in the genesis of these profiles. In addition to the hydromorphic condition related to the P1 concave pedoform, the establishment of colder climatic conditions appears to have aided the commencement of the formation of organic deposits, which are the parent materials in the genesis of Histosols. This result is like that found by Silva Neto et al. (2019), reconstructing the evolutionary trajectory of the formation of Histosols in an upper montane environment in the State of Espírito Santo, southeastern of Brazil. According to Schaefer (2013), Gleysols and Histosols at high landscape positions in southeastern region of Brazil are evidence of a past humid phase during the Holocene, with higher hydromorphism than at the present time. This phenomenon can be explained by both drainage fitting, resulting from the lowering of the base level in glacial periods, and Neotectonic uplift.

In profile P2, despite the backslope position, the dense vegetation of Atlantic Forest growing during this period stabilized the slope, contributing to the profile pedogenesis, and to the formation of a thick umbric surface horizon. In Brazil, soils with umbric horizon are found in the South and Southeast regions (humid tropical and/ subtropical environments) and are commonly associated with mountain environments (Ker, 1997, Calegari, 2008). Several studies were made to understand the development of these soil horizons, especially in weathered soils such as Ferralsols. According to Lepsch and Buol (1986), Umbric Ferralsols of the South and Southeast regions of Brazil may be in fact Paleosols, that is soils formed during the Holocene under more favorable conditions for SOM accumulation.

The occurrence of more humid and colder climatic conditions in the Holocene is also shown by paleoecologic records from other Southeastern Brazil states (Behling, 2002). In the State of Minas Gerais (MG), it was observed in the Serra do Espinhaço Meridional a period of reduced erosion occurred from −2200 to −1160 cal. yr BP, with periods of sporadic cooling accompanied by variations in humidity (Horak-Terra et al., 2014). In the same state, Ledru (1993) recorded in the Serra do Salitre semideciduous forest expansion from 4750 to 3350 cal. yr BP. In Lago do Pires (Minas Gerais State), Behling (1995) documented a dense and closed semideciduous forest expansion due to wetter conditions, approximately 1000 cal. yr BP. More humid conditions are indicated by reduction of high-altitude grasslands and expansion of Atlantic Forest in the Serra dos Órgãos (Rio de Janeiro State) (Behling and Safford, 2010). The occurrence of a period of higher humidity during the Holocene is also shown in the upper Quaternary allostratigraphic classification in Bananal region (São Paulo State). In this region, integrated dynamics of hillsides and channeled flows are documented in the zones between the hillside segments and river terraces (ramp-flat zones). Such dynamics have significant spatio-temporal discontinuities in the Holocene (Moura and Mello, 1991).

In the P3, located at the footslope, in addition to climatic effects, the growth of dense vegetation during this period may explain the relatively dark color of the subsurface horizons. The morphology of the subsurface horizons resembles that of buried A horizons or sombric horizons (IUSS Working Group WRB, 2015). However, there were no characteristics indicating lithological discontinuity in P3 darker horizons, and they did not meet the definition of a sombric horizon. Although, the processes involved in the accumulation of organic residues in the sombric horizons, as well as the criteria used for distinction, are not yet properly established (Almeida et al., 2009; Chiapini et al., 2018). In our study, the hypothesis of Caner et al. (2003) that the SOM of the dark subsurface horizons would come from past vegetations, different from the present one, being the result of eventual paleoclimatic changes, seems to be more adequate.

The pattern in soil phytolith composition in P3 indicates a very effective mixing of soil. Although several processes can modify the distribution of phytoliths in soil after their deposition, bioturbation is the only process likely to be capable of causing the massive translocation of phytoliths (Zangerlé et al., 2016). Bioturbation is acknowledged to be an important mechanism influencing the distribution of phytoliths in soils (Fishkis et al., 2010). In addition to the higher amount of weathered material in the footslope position of the toposequence, the increase in humidity promoted the relatively slow development of denser vegetation, thereby increasing the biological activity and the predominance of pedogenesis over morphogenesis. Furthermore, the water availability augmented, increasing the chemical weathering. Some studies have shown that the umbric horizons genesis may be influenced positively by the transport and deposition of materials (colluvium) from higher sections of the landscape (Lepsch and Buol, 1986; Silva and Vidal-Torrado, 1999), in addition to biological mixing promoted by soil fauna, and decomposition and migration of humic substances along the profile (Silva and Vidal-Torrado, 1999; Calegari et al., 2013a). All those theories apply to profile P3 (Umbric Ferralsol)

Phase III (after −2063 cal. yr BP) corresponds to a period of establishment of the current climate conditions (Cwb - subtropical highland climate, with dry winters and cool summers) from the Upper Holocene, corroborating the comprehensive overview of Brazilian paleoclimates in the Southern and Southeastern regions conducted by Behling (2002). During this period, phytolith records show reduced tree cover (D/P ~ 30%), which is also reflected in the isotopic composition. The organic horizons of profile P1 and the umbric horizons of P2 and P3 would have formed under the *Cwb* climate conditions, in the Upper Holocene. These results are in line with studies on the genesis and paleoenvironmental significance of umbric horizons in the Southeast region of Brazil. Isotopic ($\delta^{13}C$ and ^{14}C) and phytolithic studies by Calegari (2008) showed that the SOM in the umbric horizon of Ferralsols, in the Southeast region of Brazil, has been incorporated since the Upper Holocene. Marques (2009) suggested that the high plant biomass production and SOM accumulation observed in the formation of these soil horizons could have resulted primarily from paleoclimate changes during the Quaternary.

In the studied soils, the phytolithic and isotopic ($\delta^{13}C$) analyses were good markers of changes in climatic conditions during their pedogenesis. This further emphasizes that the identification of soil phytolith assemblages is a valuable source of paleoclimate information that can improve our understanding of soil-landscape relationships. However, in the paleopedological studies soil should be regarded as a complex and open system that evolves in space and time, and not as a simple sedimentary sequence, i.e., the addition, loss, transformation and translocation processes must be analyzed together. Many tropical soils are considerably deep, developed over pre-weathered parent materials, mainly sediments, and were formed during a long pedogeomorphological history, with significant climatic and ecological changes with the geological periods, epochs and ages. In turn, the soil properties directly affect the mechanisms of erosion and deposition occurring in the hillsides, subsequently affecting current landscape-shaping processes (Anjos et al., 1998).

Upper montane regions with strongly undulating terrain, under seasonal climate conditions, such as those observed in our study, in the Mantiqueira Range, often show stronger morphogenesis compared to pedogenesis. Soils result from the interactions between factors and processes active in different landscapes; as landscapes change, so do the soil profiles associated with them (Ladeira, 2010).

Analysis of the pedological cover in different scales complement each other and show the polygenetic formation of the studied profiles. The multiproxy approach provided important information of the paleoenvironmental conditions during the pedogenesis process, allowing to establish pedochronostratigraphic correlations, that improved the understanding of soil-landscape relationships in these environments. Soil-preserved phytolith assemblages, isotopic composition ($\delta^{13}C$) and organic matter dating (^{14}C) indicated variations in the type of plant communities in the studied soils, suggesting climatic changes that influenced soil formation and evolution.

5. Conclusions

The soils studied in the highlands of Mantiqueira Range, in Espírito Santo State, are characterized by their high SOM contents, due to the relatively cold and humid climate typical of these upland environments. The morphological differences and the evolution of the soils were conditioned mainly by variations in topography and parent materials; however, the variation of organisms and climate along the time, strongly influenced the SOM content and the formation of histic (P1) and umbric horizons (P2 and P3).

The studied soils experienced different pedogenesis conditions during the Late Holocene, and are, therefore, considered polygenetic soils. In summary, 3 phases were identified by multiproxy analysis: **Phase I** (before −2330 cal. yr BP), hotter and drier than the current period; **Phase II** (from −2330 to −2063 cal. yr BP), colder and wetter than the current period; **Phase III** (after −2063 cal. yr BP), during which the current climate conditions were established.

References

Albert, R.M., Weiner, S., 2001. Study of phytoliths in prehistoric ash layers from Kebara and Tabun caves using a quantitative approach. In: Meunier, J., Colin, F. (Eds.), Phytoliths: Applications in Earth Sciences and Human History. Balkema, Rotterdam, pp. 251–266.

Alexandre, A., Meunier, J.D., Colin, F., Koud, J.M., 1997. Plant impact on the biogeochemical cycle of silicon and related weathering processes. Geochem. Cosmochim. Acta 61 (3), 677–682. https://doi.org/10.1016/S0016-7037(97)00001-X.

Alexandre, A., Meunier, J.D., Mariotti, A., Soubies, F., 1999. Late Holocene phytolith and carbon-isotope record from a Latosol at Salitre, south-central Brazil. Quat. Res. 51, 187–194. https://doi.org/10.1006/qres.1998.2027.

Almeida, J.A., Cararo, D.C., Uberti, A.A.A., 2009. Genesis of the sombric horizon in Ultisols (Red Argisols) in southern Santa Catarina. Brazil. Rev. Bras. Ciênc. Solo 33 (2), 405–416. https://doi.org/10.1590/S0100-06832009000200018.

Alvares, C.A., Stape, J.L., Sentelhas, P.C., Gonçalves, J.L.M., Sparovek, G., 2013. Köppen's climate classification map for Brazil. Meteorol. Z. 22, 711–728. https://doi.org/10.1127/0941-2948/2013/0507.

Anjos, L.H., Fernandes, M.R., Pereira, M.G., Franzmeier, D.P., 1998. Landscape and Pedogenesis of an Oxisol-Inceptisol-Ultisol Sequence in Southeastern Brazil. Soil Sci. Soc. Am. J. 62 (6), 1651–1658. https://doi.org/10.2136/sssaj1998.03615995006200060024x.

Barboni, D., Bremond, L., Bonnefille, R., 2007. Comparative study of modern phytolith assemblages from inter-tropical Africa. Palaeogeogr. Palaeoclimatol. Palaeoecol. 246, 454–470. https://doi.org/10.1016/j.palaeo.2006.10.012.

Behling, H., 1995. A high resolution Holocene pollen record from Lago do Pires, SE Brazil: Vegetation, climate and fire history. J. Paleolimnol. 14, 253–268. https://doi.org/10.1007/BF00682427.

Behling, H., Lichte, M., 1997. Evidence of dry and cold climatic conditions at glacial times in tropical Southeastern Brazil. Quat. Res. 48, 348–358. https://doi.org/10.1006/qres.1997.1932.

Behling, H., 2002. South and southeast Brazilian grasslands during Late Quaternary times: a synthesis. Palaeogeogr. Palaeoclimatol. Palaeoecol. 177 (1–2), 19–27. https://doi.org/10.1016/s0031-0182(01)00349-2.

Behling, H., Safford, H.D., 2010. Late-glacial and Holocene vegetation, climate and fire

dynamics in the Serra dos Órgãos, Rio de Janeiro State. SE Brazil. Global Change Biology 16, 1661–1671. https://doi.org/10.1111/j.1365-2486.2009.02029.x.
Boulet, R., 1978. Toposéquences de sols tropicaux en Haute Volta: équilibres et déséquilibres pédobioclimatiques. Mémoires Orstom 85, 1–272.
Boutton, T.W., Archer, S.R., Midwood, A.J., Zitzer, S.F., Bol, R., 1998. δ^{13}C values of soil organic carbon and their use in documenting vegetation change in a subtropical savanna ecosystem. Geoderma 82, 5–41. https://doi.org/10.1016/S0016-7061(97)00095-5.
Bremond, L., Alexandre, A., Hély, C., Guiot, J., 2005. A phytolith index as a proxy of tree cover density in tropical areas: calibration with Leaf Area Index along a forest–-savanna transect in southeastern Cameroon. Glob. Planet. Chang. 45 (4), 277–293. https://doi.org/10.1016/j.gloplacha.2004.09.002.
Brown, G., Brindley, G.W., 1980. X-ray Diffraction procedures for clay mineral identification. In: Brindley, G.W., Brown, G. (Eds.), Crystal structures of clay minerals and their Xray identification. Mineralogical Society, London, pp. 305–360.
Buol, S.W., Southard, R.J., Graham, R.C., McDaniel, P.A., 2011. Soil genesis and classification, 6 Ed. Willey-Blackwell, Chichester.
Calegari, M.R., 2008. Ocorrência e significado paleoambiental do horizonte A húmico em latossolos. ESALQ, University of São Paulo, Piracicaba.
Calegari, M.R., Madella, M., Vidal-Torrado, P., Pessenda, L.C.R., Marques, F.A., 2013a. Combining phytoliths and soil organic matter in Holocene palaeoenvironmental studies of tropical soils: the example of an oxisol in Brazil. Quat. Int. 287, 47–55. https://doi.org/10.1016/j.quaint.2011.11.012.
Calegari, M.R., Madella, M., Vidal-Torrado, P., Otero, X.L., Macias, F., Osterrieth, M., 2013b. Opal phytolith extraction in oxisols. Quat. Int. 287, 56–62. https://doi.org/10.1016/j.quaint.2011.11.005.
Campos, J.R.R., Silva, A.C., Nanni, M.R., Santos, M., Vidal-Torrado, P., 2017. Influence of the structural framework on peat bog distribution in the tropical highlands of Minas Gerais, Brazil. Catena 156, 228–236. https://doi.org/10.1016/j.catena.2017.04.018.
Caner, L., Toutain, F., Bourgeon, G., Herbillon, A.J., 2003. Occurrence of sombric-like subsurface A horizons in some andic soils of the Nilgiri Hills (Southern India) and their palaeoecological significance. Geoderma 117, 251–265. https://doi.org/10.1016/S0016-7061(03)00127-7.
Chiapini, M., Schellekens, J., Calegari, M.R., Almeida, J.A., Buurman, P., Camargo, P.B., Vidal-Torrado, P., 2018. Formation of black carbon rich 'sombric' horizons in the subsoil: a case study from subtropical Brazil. Geoderma 314, 232–244. https://doi.org/10.1016/j.geoderma.2017.10.031.
Curi, N., Franzmeier, D.P., 1984. Toposequence of Oxisols from the Central plateau of Brazil. Soil Sci. Soc. Am. J. 48, 341–346. https://doi.org/10.2136/sssaj1986.03615995005000040034x.
Delhon, C., 2005. Anthropisation et paleoclimats du Tardiglaciaire k l'Holocene en moyenne vallee du Rhone: estudes pluridisciplinaires des spectres phytolithiques et pedo-anthracologiques de sequences naturelles et de sites archeologiques. Tese. Universite Paris, Paris.
Fishkis, O., Ingwersen, J., Lamers, M., Denysenko, D., Streck, T., 2010. Phytolith transport in soil: a field study using fluorescent labelling. Geoderma 157, 27–36. https://doi.org/10.1016/j.geoderma.2010.03.012.
Gražulis, S., Chateigner, D., Downs, R.T., Yokochi, A.F.T., Quirós, M., Lutterotti, L., Le Bail, A., 2009. Crystallography Open Database–an open-access collection of crystal structures. J. Appl. Crystallogr. 42 (4), 726–729. https://doi.org/10.1107/S0021889809016690.
Grimm, E.C., 1987. CONISS: A Fortran 77 program for stratigraphically constrained cluster analysis by the method of the incremental sum of squares. Comput. Geosci. 13, 13–35. https://doi.org/10.1016/0098-3004(87)90022-7.
Hallett, R.B., Kyle, P.R., 1993. XRF and INAA determinations of major and trace elements in geological survey of Japan igneous and sedimentary rock standards. Geostandards Newsletter 17, 127–133. https://doi.org/10.1111/j.1751-908X.1993.tb00128.x.
Horak-Terra, I., Cortizas, A.M., Camargo, P.B., Silva, A.C., Vidal-Torrado, P., 2014. Characterization of properties and main processes related to the genesis and evolution of tropical mountain mires from Serra do Espinhaço Meridional, Minas Gerais, Brazil. Geoderma 234, 183–197. https://doi.org/10.1016/j.geoderma.2014.05.008.
Horak-Terra, I., Martínez-Cortizas, A., Luz, C.F.P., Rivas-López, P., Silva, A.C., Vidal-Torrado, P., 2015. Holocene climate change in central-eastern Brazil reconstructed using pollen and geochemical records of Pau de Fruta mire (Serra do Espinhaço Meridional, Minas Gerais). Palaeogeogr. Palaeoclimatol. Palaeoecol. 437, 117–131. https://doi.org/10.1016/j.palaeo.2015.07.027.
IUSS Working Group WRB, 2015. World Reference Base for Soil Resources 2014, update 2015. International soil classification system for naming soils and creating legends for soil maps (World Soil Resources Reports no. 106), FAO, Rome.
Jackson, M.L., 1975. Soil Chemical Analysis: Advance Course, second ed. Parallel Press, Madison.
Jahn, R., Blume, H.P., Asio, V.B., Spaargaren, O., Schad, P., 2006. Guidelines for Soil Description. FAO, Rome.
Janzen, H.H., 2016. The soil remembers. Soil Sci. Soc. Am. J. 80 (6), 1429–1432. https://doi.org/10.2136/sssaj2016.05.0143.
Johnson, D.L., Watson-Stegner, D., 1987. Evolution model of pedogenesis. Soil Sci. 143, 349–366. https://doi.org/10.1097/00010694-198705000-00005.
Juggins, S., 2007. C2 Version 1.5 User Guide. Software for Ecological and Palaeoecological Data Analysis and Visualisation. Newcastle University, Newcastle upon Tyne, Newcastle.
Kämpf, N., Marques, J.J., Curi, N., 2012. Mineralogia dos solos brasileiros. In: Ker, J.C., Curi, N., Schaefer, C.E.G.R., Vidal-Torrado, P. (Eds.), Pedologia: fundamentos. Sociedade Brasileira de Ciência do Solo, Viçosa, pp. 81–145.
Ker, J.C., 1997. Latossolos do Brasil: uma revisão. Geonomos 5, 17–40. https://doi.org/10.18285/geonomos.v5i1.187.
Kroetsch, D.J., Geng, X., Chang, S.X., Saurette, D.D., 2011. Organic soils of Canada: Part 1. Wetland organic soils. Can. J. Soil Sci. 91 (5), 807–822. https://doi.org/10.4141/cjss10043.
Ladeira, F.S.B., 2010. Soils of the past: origin and identity. Rev. Bras. Ciênc. Solo 34 (6), 1773–1786. https://doi.org/10.1590/S0100-06832010000600001.
Ledru, M.P., 1993. Late Quaternary environmental and climatic changes in Central Brazil. Quat. Res. 39, 90–98. https://doi.org/10.1006/qres.1993.1011.
Lepsch, I.F., Buol, S.W., 1986. Oxisol-landscape relationship in Brazil, in: International Soil Classification Work Shop, Campinas. University of Puerto Rico, pp. 174-189.
Marques, F.A., 2009. Matéria orgânica de Latossolos com horizonte A húmico. ESALQ, University of São Paulo, Piracicaba.
Messager, E., Lordkipanidze, D., Delhon, C., Ferring, C.R., 2010. Palaeoecological implications of the Lower Pleistocene phytolith record from the Dmanisi Site (Georgia). Palaeogeogr. Palaeoclimatol. Palaeoecol. 288, 1–13. https://doi.org/10.1016/j.palaeo.2010.01.020.
Milnes, A.R., Fitzpatrick, R.W., 1989. Titanium and zirconium minerals. In: Dixon, J.B., Weed, S.B. (Eds.), Minerals in Soil Environment. Soil Science Society America, Madison, pp. 1131–1205.
Moore, D.M., Reynolds, R.C., 1989. X-ray Diffraction and the Identification and Analysis of Clay Minerals. Oxford University Press, New York, NY, USA.
Moura, J.R.S., Mello, C.L., 1991. Classificação aloestratigráfica do Quaternário superior na região de Bananal (SP). Revista Brasileira de Geociências 21 (3), 236–254. https://doi.org/10.20396/rap.v9i3.8641304.
Nehren, U., Kirchner, A., Heinrich, J., 2016. What do yellowish-brown soils and stone layers tell us about Late Quaternary landscape evolution and soil development in the humid tropics? A field study in the Serra dos Órgãos, Southeast Brazil. Catena 137, 173–190. https://doi.org/10.1016/j.catena.2015.09.016.
Neumann, K., Strömberg, C.A.E., Ball, T., Albert, R.M., Vrydaghs, L., Cummings, L.S., 2019. International Code for Phytolith Nomenclature (ICPN) 2.0. Ann. Bot. 124 (2), 189–199. https://doi.org/10.1093/aob/mcz064.
Pereira, N.V., Safford, H.D., Behling, H., 2012. Holocene vegetation and fire history of the Serra do Caparaó, SE Brazil. The Holocene 22 (11), 1243–1250. https://doi.org/10.1177/0959683612437864.
Pessenda, L.C.R., 1996. The use of carbon isotopes (^{13}C, ^{14}C) in soil to evaluate vegetation changes during the Holocene in Central Brazil. Radiocarbon 38, 191–201. https://doi.org/10.1017/S0033822200017562.
Pinheiro, M.R., Queiroz Neto, J.P., 2017. From the semiarid landscapes of southwestern USA to the wet tropical zone of southeastern Brazil: Reflections on the development of cuestas, pediments, and talus. Earth Sci. Rev. 172, 27–42. https://doi.org/10.1016/j.earscirev.2017.07.005.
Piperno, D.R., 2006. Phytoliths: A Comprehensive Guide for Archaeologists and Paleoecologists. Lanham MD - AltaMira Press, San Diego.
Rashid, I., Mir, S.H., Zurro, D., Dar, R.A., Reshi, Z.A., 2019. Phytoliths as proxies of the past. Earth Sci. Rev. 194, 134–250. https://doi.org/10.1016/j.earscirev.2019.05.005.
Reimer, P.J., Bard, E., Bayliss, A., Beck, J.W., Blackwell, P.G., Bronk Ramsey, C., Buck, C.E., Cheng, H., Edwards, R.L., Friedrich, M., Grootes, P.M., Guilderson, T.P., Haflidason, H., Hajdas, I., Hatté, C., Heaton, T.J., Hoffman, D.L., Hogg, A.G., Hughen, K.A., Kaiser, K.F., Kromer, B., Manning, S.W., Niu, M., Reimer, R.W., Richards, D.A., Scott, E.M., Southon, J.R., Staff, R.A., Turney, C.S.M., van der Plicht, J., 2013. IntCal13 and Marine 13 radiocarbon age calibration curves 0–50,000 years cal BP. Radiocarbon 55, 1869–1887. https://doi.org/10.2458/azu_js_rc.55.16947.
Ruhe, R.V., Olson, C.G., 1980. Soil welding. Soil Sci. 130 (3), 132–139. https://doi.org/10.1007/978-90-481-3585-1_825.
Santos, H.G., Jacomine, P.K.T., Anjos, L.H.C., Oliveira, V.A., Lumbreras, J.F., Coelho, M.R., Almeida, J.A., Cunha, T.J.F., Oliveira, J.B., 2018. Sistema Brasileiro de Classificação de. Solos, Brasília.
Schaefer, C.E.R., 2001. Brazilian latosols and their B horizon microstructure as long-term biotic constructs. Aust. J. Soil Res. 39, 909–926. https://doi.org/10.1071/SR00093.
Schaefer, C.E.G.R., 2013. Bases Físicas da Paisagem Brasileira: Estrutura Geológica, Relevo e Solos. Tópicos em Ciência do Solo 8, 221–278.
Schaetzl, R.J., 1998. Lithologic discontinuities in some soils on drumlins. Theory, detection, and application. Soil Sci. 163, 570–590. https://doi.org/10.1097/00010694-199807000-00006.
Simas, F.N.B., Schaefer, C.E.G.R., Fernandes, E.I., Chagas, A.C., Brandão, P.C., 2005. Chemistry, mineralogy and micropedology of highland soils on crystalline rocks of Serra da Mantiqueira, southeastern Brazil. Geoderma 125, 187–201.
Silva Neto, E.C., Calegari, M.R., Pereira, M.G., Maranhão, D.D.C., Schiavo, J.A., Fontana, A., Fernandes, J.C.F., 2018a. Phytoliths as indicators of pedogenesis and paleoenvironmental changes in Spodosols of the state of Rio de Janeiro, Brazil. Sci. Total Environ. 636, 1070–1080.
Silva Neto, E.C., Santos, J.J.S., Pereira, M.G., Maranhão, D.D.C., Barros, F.D.C., Anjos, L.H.C., 2018b. Paleoenvironmental Characterization of a High-Mountain Environment in the Atlantic Forest in Southeastern Brazil. Revista Brasileira de Ciência do Solo 42 (1–17), 2018.
Silva Neto, E.C., Pereira, M.G., Carvalho, M.A., Calegari, M.R., Schiavo, J.A., Sa, N.P., Anjos, L.H.C., Pessenda, L.C.R., 2019. Palaeoenvironmental records of Histosol pedogenesis in upland area, Espírito Santo State (SE, Brazil). J. S. Am. Earth Sci. 95, 1–12. https://doi.org/10.1016/j.jsames.2019.102301.
Silva, A.C., Vidal-Torrado, P., 1999. Gênese dos Latossolos Húmicos e sua relação com a evolução da paisagem numa área cratônica do sul de Minas Gerais. Rev. Bras. Ciênc. Solo 23, 329–341. https://doi.org/10.1590/S0100-06831999000200017.
Taboada, T., Cortizas, A.M., Garcia, C., Rodeja, E.G., 2006. Particle-Size Fractionation of Titanium and Zirconium during Weathering and Pedogenesis of Granitic Rocks in NW Spain. Geoderma 131 (2), 218–236. https://doi.org/10.1016/j.geoderma.2005.03.025.
Targulian, V.O., Bronnikova, M.A., 2019. Soil memory: theoretical basics of the concept,

its current state, and prospects for development. Eurasian Soil Sci. 52 (3), 229–243. https://doi.org/10.1134/S1064229319030116.
Targulian, V.O., Goryachkin, S.V., 2011. Soil memory and environmental reconstructions. Eurasian Soil Science. 44 (4), 464–465. https://doi.org/10.1134/S1064229311040119.
Teixeira, P.C., Donagemma, G.K., Fontana, A., Teixeira, W.G., 2017. Manual de métodos de análise de solo. Embrapa, Brasília.
Tsai, C., Chen, Z., 2000. Lithologic discontinuities in Ultisols along a toposequence in Taiwan. Soil Sci. 165, 587–596. https://doi.org/10.1097/00010694-200007000-00007.
Twiss, P.C., 1992. Predicted world distribution of C_3 and C_4 grass phytoliths. In: Rapp, G., Mulholland, S.C. (Eds.), Phytolith Systematics. Emerging Issues, Advances in Archeological and Museum Science. Plenum Press, pp. 113–128.
USDA, 1975. Soil Taxonomy. Agriculture Handbook. United States Department of Agriculture/Pocahontas Press, Washington.
van Breemen, N., Buurman, P., 2002. Soil Formation, second ed. Kluwer Academic Publishers, Amsterdam.
Vidal-Torrado, P., Lepsch, I.F., Castro, S.S., 2005. Conceitos e Aplicações das Relações Pedologia-Geomorfologia em Regiões Tropicais Úmidas. Tópicos em Ciências do Solo 4, 145–192.
Vieira, B.C., Gramani, M.F., 2015. Serra do Mar: The Most “Tormented” Relief in Brazil. In: Vieira, B.C., Salgado, A.A.R., Santos, L.J.C. (Eds.), Landscapes and Landforms in Brazil. Springer, New York, pp. 285–299.
Zangerlé, A., Renard, D., Iriarte, J., Suarez Jimenez, L.E., Adame Montoya, K.L., Juilleret, J., McKey, D., 2016. The surales, self-organized earth-mound landscapes made by earthworms in a seasonal tropical wetland. PLoS ONE 11 (5), 1–33. https://doi.org/10.1371/journal.pone.0154269.